RSC Sustainability

ROYAL SOCIETY OF CHEMISTRY

TUTORIAL REVIEW

View Article Online
View Journal | View Issue

Cite this: *RSC Sustainability*, 2025, **3**, 2160

MXene-based nanocomposites: a new horizon for electrochemical monitoring of environmental pollutants

Ali Hyder,[a] Meher-Un-Nisa Khilji,[a] Jamil A. Buledi,[a] Ayaz Ali Memon,*[a] Azharuddin Ghanghro,[a] Misbah ur Rehman[b] and Khalid Hussain Thebo *[c]

MXenes, two-dimensional (2D) transition metal carbides and nitrides, have garnered attention due to their outstanding electrical conductivity, expansive surface area, and customizable surface chemistry and have been widely investigated for use in environmental sensors in recent years. This review presents a variety of methodologies for synthesizing MXene-based nanocomposites and their utilization as electrochemical sensors for the detection of environmental pollutants, including organic pesticides, antibiotic drugs, heavy metals, and synthetic phenolic compounds in real matrices. The review includes various synthesis approaches, which include a spectrum of techniques, such as chemical etching, intercalation, and surface modification, all directed at tailoring the properties of MXenes to optimize sensor functionality. Subsequently, the role of these MXene-based nanocomposites in electrochemical sensing will be discussed in detail. These sensors demonstrate exceptional sensitivity, selectivity, and swift responsiveness, positioning them as promising contenders for on-the-spot monitoring of pollutants. The specific emphasis on heavy metals tackles the pervasive concern of water contamination, while the identification of organic pesticides and antibiotic drugs addresses issues in agricultural and pharmaceutical wastewater. The electrochemical sensing capacities of MXene-based nanocomposites offer promising prospects for effective and portable devices for environmental monitoring. We believe this review will provide new ideas and research directions for readers working with sensor-based technologies.

Received 29th December 2024
Accepted 28th March 2025

DOI: 10.1039/d4su00828f

rsc.li/rscsus

[a]*National Centre of Excellence in Analytical Chemistry, University of Sindh, Jamshoro 76080, Pakistan. E-mail: ayazmemon33@usindh.edu.pk*
[b]*Department of Chemistry, University of Mianwali, Mianwali 42200, Pakistan*
[c]*Institute of Metal Research (IMR), Chinese Academy of Science, 2 Wenhua Rood, Shenyang, China. E-mail: khalidthebo@yahoo.com*

Ali Hyder

Dr Ali Hyder is a PhD researcher specializing in calixarene-functionalized 2D nanomaterials. His research focuses on the applications of 2D materials in adsorption, membrane separation, and electrochemical sensors. His work significantly contributes to advancing the practical applications of nanotechnology. With a keen interest in materials science, his expertise lies in harnessing the unique properties of nanomaterials for diverse technological solutions. Through meticulous research and innovation, Ali continues to make remarkable strides in the field of nanotechnology.

Meher-Un-Nisa Khilji

Meher-Un-Nisa Khilji received her MS in biochemistry and clinical biochemistry from Shah Abdul Latif University, Khairpur Mirs, Sindh, Pakistan. She later earned her PhD in analytical chemistry in 2023 from the National Centre of Excellence in Analytical Chemistry, Sindh University, Jamshoro, under the supervision of Dr Ayaz Ali Memon and Dr Khalid Hussain Thebo. She has extensive expertise in material chemistry, particularly in the synthesis of 2D materials and their applications in environmental science.

Sustainability spotlight

The increasing contamination of environmental matrices by toxic pollutants has become a pressing global health concern. To address this issue, the development of sophisticated monitoring technologies is essential for the precise detection of antibiotics, toxic compounds, and other pollutants in real-time, particularly in complex environmental and biological systems. Recently, two-dimensional transition metal carbides and nitrides (MXenes), known for their exceptional electrical conductivity and high surface area, have been widely investigated for environmental sensing applications. This review provides a comprehensive overview of the synthesis methodologies for MXene-based nanocomposites and their applications as electrochemical sensors for detecting various environmental pollutants, including pesticides, antibiotics, heavy metals, and phenolic compounds.

Jamil A. Buledi

Dr Jamil A. Buledi, a distinguished researcher, has made significant contributions to the scientific community through his extensive publication record. With over 50 research articles in esteemed international journals, his work has garnered widespread recognition, accumulating an impressive 203.73 IF, showcasing the depth of his influence in his field. Notably, he has been honored as a highly cited scientist in the Journal of Electroanalysis, solidifying his reputation as a leader in his field. Dr Buledi's dedication to advancing knowledge through research underscores his commitment to scientific excellence and innovation.

Ayaz Ali Memon

Ayaz Ali Memon is an Associate Professor at the National Centre of Excellence in Analytical Chemistry (NCEAC), University of Sindh Jamshoro, with expertise and experience in basic, analytical, material, and environmental chemistry. Dr Memon earned his PhD in analytical chemistry in 2012 from the University of Sindh Jamshoro. He has published 85 peer-reviewed articles. His research interests include basic experiments such as the synthesis of nanoparticles and GO, membrane preparation, surface functionalization, characterizations, and project management.

Azharuddin Ghanghro

Mr Azharuddin Ghanghro is a distinguished researcher and scholar at NCEAC, University of Sindh Jamshoro, Pakistan. He completed his MPhil degree from NCEAC, University of Sindh Jamshoro, Pakistan. He has extensive experience in synthesizing nanofibers and non-conductive nanofibers for various biochemical applications.

1. Introduction

Nowadays, the rapid pace of industrialization has led to the release of various pollutants into water bodies without adequate treatment, resulting in severe environmental contamination and posing significant risks to human health.[1–3] Moreover,

Misbah ur Rehman

Dr Misbah is currently serving as an Associate Professor in the Department of Chemistry at the University of Lahore, Sargodha Campus, Sargodha, Pakistan. He completed his PhD degree from BZU University, Multan, and the University of Manchester, UK. His research interests include the synthesis of nanomaterials for drinking water purification, desalination, and photocatalysis.

Khalid Hussain Thebo

Dr Khalid Hussain Thebo completed his MPhil at the School of Chemistry, University of Manchester (UoM), United Kingdom, under the supervision of Prof. Paul O'Brien (late). Dr Thebo then earned his PhD in material chemistry from the Institute of Metal Research, Chinese Academy of Sciences (CAS), China, under the supervision of Prof. Wencai Ren and Prof. Hui-Ming Cheng. His doctoral research focused on "graphene-based membranes for water purification and desalination applications". His research interests include the synthesis of 2D materials (graphene, MXene, and metal chalcogenides), membrane science and technology for drinking water purification and wastewater reuse, gas membranes, proton exchange membranes, and photocatalysis.

various industrial sectors have discharged numerous containments into aqueous environments without proper treatment.[4–7] Among various pollutants, certain substances, such as heavy metal ions, pharmaceutical compounds, synthetic phenolic compounds, and pesticides, have the potential to create severe environmental issues and lead to harmful effects on aquatic life.[8–13] These pollutants can disrupt ecosystems and have wide-ranging consequences for aquatic organisms and the environment.[14,15] Toxic heavy metals, especially cadmium, lead, chromium, copper, and mercury, can pose significant risks to both the environment and human health, even at trace levels.[16–18] These metals are known for their harmful effects, and their presence, even in small amounts, can have serious consequences on human health, such as eye injuries, skin irritations, respiratory tract disorders, vomiting, dizziness, mutagenic effects, teratogenicity (causing birth defects), and gastrointestinal complications.[19] Apart from heavy metal ions, synthetic organic compounds, such as pharmaceuticals, phenolic compounds, and pesticides, persist in the environment long after their use, leaving residues that can endure for extended periods.[20–23] The difficulty in breaking down the aromatic ring structure contributes to the environmental persistence of these compounds.[24,25] Therefore, the residues of these pollutants can enter water bodies and the food chain through various environmental pathways. This contamination can have adverse effects on human health, potentially leading to conditions such as anemia.[26,27] Therefore, the presence and persistence of these substances in the environment pose health risks and emphasize the importance of effective monitoring and control measures to minimize their impact on human health.

To date, various conventional methods have been applied for the removal of these environmental pollutants from wastewater systems, such as high-performance liquid chromatography, gas chromatography, inductively coupled plasma optical emission spectroscopy, UV-vis spectroscopy, colorimetric sensors, and fluorescent sensors.[28–33] However, these conventional methods have several drawbacks including requirement of skilled technicians and complex and costly equipment, use of toxic solvents and multi-step detection procedures for the determination of pollutant compounds from real matrices. Alternatively, electrochemical sensors have gained significant research attention due to their advantages in terms of simplicity, rapid response, ease of adaptation into portable equipment, high selectivity and sensitivity towards the desired analyte from real matrices.[34–38] In this case, various functionalized materials are used as modified electrochemical sensors such as metal and metal oxide nanoparticles, metal–organic frameworks (MOFs), graphene oxide-based nanocomposites, carbon nanotubes (CNTs) and conducting polymers for the selective detection of environmental pollutants from wastewater.[39–44] Among them, MXene-based composites have recently gained significant attention from the scientific community due to their exceptional properties.[45,46] This interest is driven by the presence of various functional terminations such as –OH, –F, and –O on the surface of MXenes, which enhance their conductive and electrical properties.[47,48]

In last few years, 2D nanomaterials have attracted increasing attention and found extensive use in various applications including energy storage devices, water purification systems, biomedical applications and sensor technology.[49,50] These materials have opened up new possibilities in a range of technological and scientific fields. MXenes, with the chemical formula $M_{n+1}X_nT_x$, are composed of transition metals including Ti, V, W, Cr, Zr, Nb, Mo, Hf, and Ta (represented as M), together with elements such as C, N, and B (represented as X), and surface functional groups such as –F, –OH, and –O (referred to as T_x).[51,52] These materials now make up a family of two-dimensional (2D) layered materials known for their remarkable properties and a wide range of potential applications.[53,54] MXenes have made a significant impact in materials chemistry research due to their exceptional and tunable intrinsic physicochemical properties, wide potential windows, chemical stability, and impressive conductivity (reaching up to 10 000 S cm^{-1} for $Ti_3C_2T_x$).[53] These attributes make them highly suitable for a wide range of applications in energy and environmental devices. MXenes have the potential to drive advancements in these areas.[55] Due to their outstanding properties including large surface area, eco-friendliness, enhanced chemical stability, hydrophilicity, and electrical/thermal conductivity, MXenes have been proven to be ideal materials for a wide array of applications including hydrogen storage, energy storage, catalysis, membrane technology and electrochemical sensors.[56–59] Various surface functionalizing agents, including polymers, organic reagents, metal and metal oxide nanoparticles, and bio-molecules, have been extensively utilized to enhance the physical and chemical properties of MXenes.[60–63] Alternatively, the etching process introduces a significant number of functional groups such as –OH, –O, and –F, which greatly enhance the hydrophilicity, biocompatibility, and functionalizability of MXenes.[64] This makes them excellent candidates as electrochemical sensor substrate materials, allowing improved sensor performances and versatility in various applications.[65]

This review article focuses on the synthesis and surface modification of MXene-based nanocomposite materials and their application in the electrochemical sensing of different environmental pollutants in real samples.

2. Fabrication of MXenes

MXenes are commonly obtained from their MAX phase precursors through a selective etching process that targets the group A elements, such as aluminum (Al) and silicon (Si). This process entails the selective elimination of the A layers from the MAX phases at room temperature. In a groundbreaking experiment, $Ti_3C_2T_x$ MXene was synthesized by selectively removing the aluminum (Al) component from the Ti_3AlC_2 MAX phase using hydrofluoric acid (HF) as the etchant.[66,67] The MAX phase powder is agitated in an aqueous solution of hydrofluoric acid (HF) for a specified duration, followed by centrifugation and multiple rinses with distilled water until the pH level stabilizes within the range of 4 to 6. The substitution of aluminum (Al) layers with Tx terminal groups such as –OH, –O, and –F signifies a sequence of chemical reactions occurring between the MXene surface and hydrofluoric acid (HF) throughout the process.[68]

Following this, the subsequent phase entails obtaining single- or few-layered, loosely packed, exfoliated graphite-like structures (MXenes) through ultrasonic delamination. Subsequently, an additional intercalation process with larger cations is employed to augment the efficiency of the overall procedure. The quality and yields of MXenes depend on various experimental factors, including the particle size of the MAX phases, temperature, etching duration, and concentration of hydrofluoric acid (HF).[69]

Recently, efforts have been devoted to substituting the hazardous hydrofluoric acid (HF), as well as other compounds such as ammonium bifluoride and fluoride salts.[70] This substitution aims to generate *in situ* HF during the etching processes of M_n+1AX_n phases. There are also reports available on fluoride-free methods for the synthesis of MXenes. MXenes present a favorable choice compared to other 2D materials due to their attributes, which include electrical conductivity, high hydrophilicity, excellent ion intercalation capabilities, and straightforward functionalization. Additionally, MXenes can be readily produced on a large scale, making them promising materials for various applications. Certainly, the combination of these properties makes MXenes excellent candidates for the development of high-performance electrochemical sensors for the monitoring of environmental pollutants in aqueous systems. Fig. 1 schematically illustrates the exfoliation process of MAX phases and the subsequent formation of MXenes.[71]

The inherent characteristics of MXenes stem from their unique compositions and structural attributes. Therefore, the structures and routes for the successful synthesis of MXenes are discussed in this section. The pioneering work of Gogotsi and Barsoum *et al.* in 2011 established hydrofluoric acid (HF) as a crucial etchant for the selective extraction of MXenes from their MAX phase precursors.[68] In 2011, Gogotsi and Barsoum *et al.* conducted groundbreaking research that identified hydrofluoric acid (HF) as a crucial etchant for selectively extracting MXenes from their MAX phase precursors. They focused on the Al atomic layers in Ti_3AlC_2 and found that the use of 50% HF played a key role in generating accordion-like $Ti_3C_2T_x$ powder. This approach capitalized on the high reactivity between Al-containing MAX phases and F ions, leading to the formation of van der Waals forces and hydrogen bonds between layers. The resulting $Ti_3C_2T_x$ powder retained the stoichiometry and crystal structure of Ti_3AlC_2 except for the absence of the Al atomic layer. Various surface terminations, such as F, OH, and O, were introduced during the aqueous etching process.[68] In a separate investigation, Alhabeb *et al.* explored the effects of the concentration of hydrofluoric acid (HF) and etching duration on Ti_3AlC_2 at room temperature.[72] Higher concentrations of HF were found to lead to shorter etching times and increased efficiency. Interestingly, the characteristic accordion-like structure, commonly observed in MXene products, did not exclusively indicate successful etching. The accordion-like structure primarily arose from the exothermic reaction during aluminum removal and the release of hydrogen gas (H_2). Additionally, the concentration of HF influenced the surface terminations, with lower concentrations favoring fluorine (–F) and oxygen-containing terminations, while higher concentrations increased the fluorine terminations and decreased the oxygen-containing terminations. A notable breakthrough in this field was the introduction of an HCl/LiF solution for etching Ti_3AlC_2 at 40 °C, as reported by Ghidiu *et al.* in 2014.[73] This technique yielded $Ti_3C_2T_x$ conductive clay with remarkable flexibility, high toughness, and favorable hydrophilicity, making it suitable for various

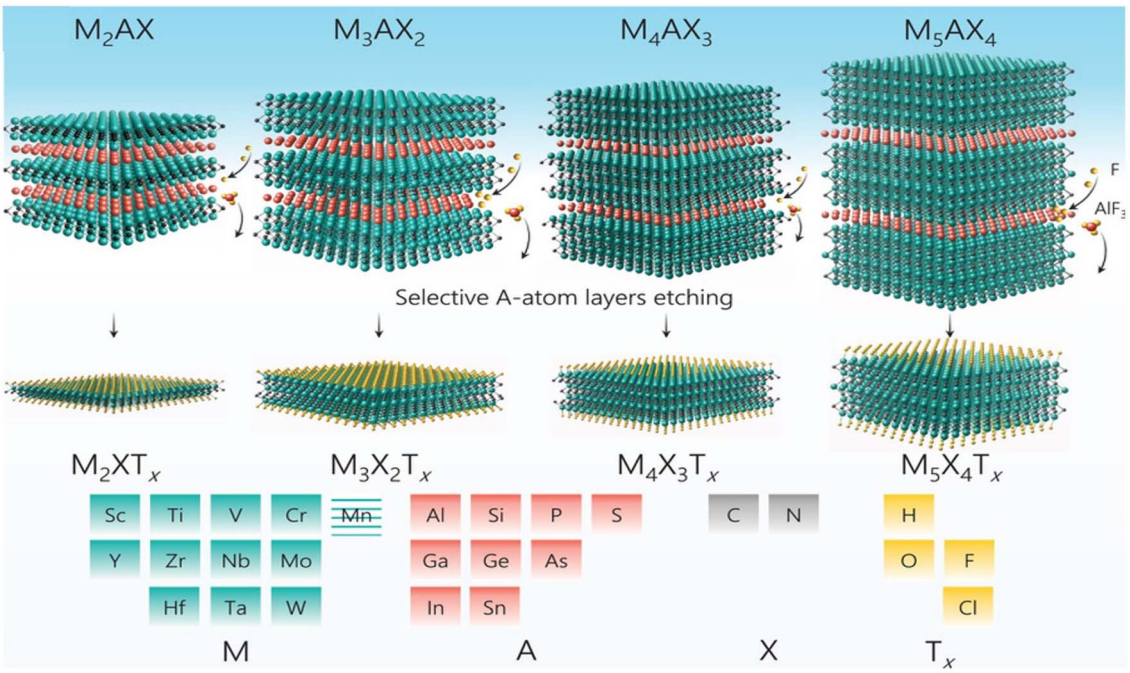

Fig. 1 MAX phases used for the synthesis of different MXene forms.[71] Copyright (2021), adopted from John Wiley and Sons.

applications, including supercapacitors. Similar to HF etching, this process resulted in the formation of multilayered accordion-like MXenes. Various fluoride salts, such as LiF, NaF, KF, and NH_4F, were integrated with HCl, offering flexibility in regulating the interlayer spacing of MXenes for specific applications. Liu *et al.* conducted an investigation into mixed solutions comprised of HCl and various fluoride salts, customizing etching parameters to produce MXenes under different temperatures and durations. The choice of mixed etchants, such as HCl/NH_4F, played a crucial role in the etching efficiency, allowing the complete transformation of Ti_3AlC_2 into $Ti_3C_2T_x$ within a short etching time of 24 h at 30 °C. Furthermore, the combination of HCl with oxidants such as FeF_3 expanded the interlayer spacing by facilitating the intercalation of Fe^{3+} ions. However, the presence of Fe^{3+} introduced challenges due to the potential oxidation of MXenes, impacting their overall yield, as shown in Fig. 2.[74] Hao *et al.* introduced a thermo-assisted electrochemical etching method without intercalators. This approach utilized a three-electrode system with 1 M HCl, Pt, and a calomel electrode serving as the electrolyte, counter electrode, and reference electrode, respectively. Various MAX phases, including Ti_3AlC_2, V_2AlC, and Cr_2AlC underwent etching. The morphology and products of Ti_2AlC_2 under different HCl concentrations, temperatures, and reaction times exhibited accordion-like structures after 3 to 9 h at 50 °C, with minimized CDC layer generation within 9 h, achieving enhanced efficiency.[75] Urbankowski *et al.* successfully achieved the etching of Ti_4AlN_3 using mixed molten salts (LiF, NaF, and KF) at 550 °C for 0.5 h, resulting in $Ti_4N_3T_x$ MXenes with an accordion-like morphology. Molten salt etching stands out as the primary method for etching high-energy barrier MAX phases such as nitrides, given that alternative approaches such as thermal treatments have proven less effective.[76]

3. Surface functionalization of MXenes

The multilayer structure of MXenes is a key characteristic, and the spacing between the layers within their structure holds significant importance in various electrochemical applications.[77] Several strategies have been proposed to increase the spacing between the layers of MXene, aiming to create single or few-layered frameworks.[78] However, the etching process typically results in the production of multilayer MXene. These multilayers are held together through the interaction of hydrogen bonding and van der Waals forces. Utilizing delamination or exfoliation techniques allows the creation of single or few-layered MXene structures.[78] Furthermore, the choice of etchant in the initial step influences the exfoliation technique. For instance, when using the LiF/HCl approach for the fabrication of MXenes, Li^+ ions intercalate between the layers. Alternatively, subjecting the material to prolonged ultrasonication or vigorous shaking can result in the generation of numerous defects, lower yields, and smaller sheets. Therefore, utilizing intercalating agents is the preferable approach to the delamination process. Additionally, intercalating agents play a crucial role in diminishing the interactions between layers and increasing the interlayer distance, ultimately leading to the formation of single or few-layered frameworks. In the case of the HF approach, exfoliation is achieved with the support of organic compounds or ions that intercalate between layers, thereby promoting an increased interlayer distance between the MXene sheets.[79] The commonly utilized intercalants include hydrazine, tetrabutylammonium hydroxide, urea, dimethylsulfoxide, isopropylamine, and tetramethylammonium hydroxide.[80] The choice of intercalant depends on the specific composition and characteristics of the MXene material being processed. These substances play a crucial role in the exfoliation process and the enhancement of the interlayer spacing in MXene materials. For instance, in a recent study, tetrabutylammonium hydroxide was selected as the intercalant for the exfoliation of $Ti_3C_2T_x$, which had been prepared through the HF etching process of the MAX phase. The MAX powder initially in the form of micro-flakes underwent expansion after the removal of aluminum (Al), resulting in Ti_3C_2–HF. Thus, this material was further delaminated into single or few-layered MXenes. The delamination process involved weakening the interactions between layers, which was achieved by utilizing tetra-butylammonium hydroxide.[81] In another study, Wang *et al.* reported a straightforward method for delaminating Ti_3C_2 with the assistance of sodium ion (Na^+) intercalation, accompanied by surface modification using aryl diazonium salts. The fundamental approach

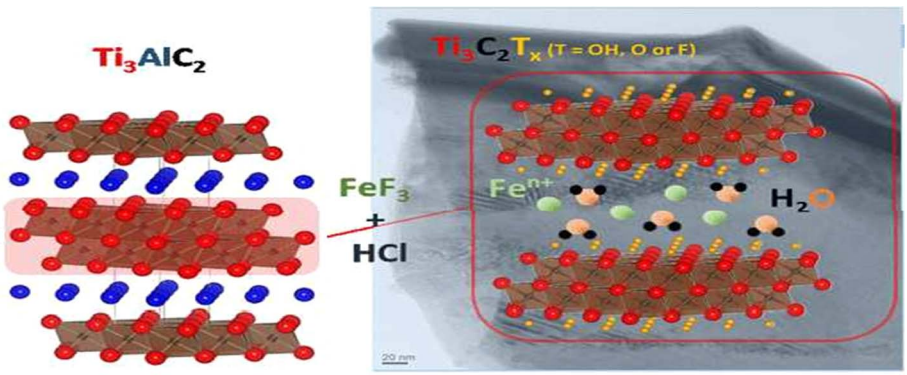

Fig. 2 Selective etching of MAX phase to produce MXene nanosheets. Reproduced from ref. 74. Copyright (2017) with permission from The Royal Society of Chemistry.

involves the synthesis of Ti_3C_2 using the HF method and subsequent intercalation with sodium ions (Na^+), and finally surface modification with sulfanilic acid diazonium salts. This sequence induces swelling and leads to the weakening of the interlayer bonds through gentle sonication. Moreover, this process involves the initial preparation of Ti_3C_2 using the HF method, followed by intercalation with sodium ions (Na^+), and subsequently surface modification through sulfanilic acid diazonium salts.[82] These steps induce swelling, which in turn weakens the bonds between the layers. Therefore, this approach serves as an alternative method for the large-scale delamination of multilayer MXenes and surface modification with aryl groups, offering opportunities for exploration in various applications. However, many of the synthetic methods discussed earlier rely on the top-down approach, wherein the bulk precursors are converted into sheet-like structures. Consequently, control of the morphology, size, and structure is often limited in these processes. Alternatively, the bottom-up approach involves the assembly of individual atoms or molecules to construct larger nanostructures. The bottom-up approach offers numerous advantages over the top-down method, including homogeneous chemical composition, reduced defects, and uniform size and shape. Consequently, bottom-up approaches are highly recommended for the preparation of MXenes and their composite materials.

Over the past few years, MXene nanostructures have found application in the creation of diverse sensing devices, including electrochemical (bio)sensors, piezoresistive wearable sensors, gas adsorptive sensors, and optical sensors, to accurately monitor numerous different matrices in aqueous medium.[83] Besides, a wide range of materials, such as enzymes, polymeric substances, graphene oxide, metal–organic frameworks, metal oxides, and metal nanoparticles, can be incorporated into MXenes to enhance their structural and electronic characteristics for different types of advanced applications. Also, the introduction of noble metal nanoparticles, such as palladium (Pd), gold (Au), and silver (Ag), on the surface of MXenes was successfully demonstrated without the use of a reducing agent. The modified MXene was further employed as a substrate for surface-enhanced Raman spectroscopy (SERS).[84] Lorencova and co-workers constructed a nanocomposite consisting of MXene and platinum nanoparticles (Pt-NPs) by reducing a platinum precursor on the surface of MXene. Subsequently, this nanocomposite was utilized in various electrochemical sensing applications. The composite produced in this manner displayed significantly improved electrochemical potential compared to the pristine MXene. This enhancement was attributed to the remarkable catalytic capability, large surface area, and excellent conductivity of the platinum nanoparticles incorporated in the composite material.[85] Furthermore, Rakhi *et al.* synthesized a novel nanocomposite by immobilizing glucose oxidase on MXene together with gold nanoparticles (Au NPs). This nanocomposite was designed for glucose sensing. The gold nanoparticles played a crucial role in facilitating the transfer of electrons between the electrode and the active sites of the enzyme, enhancing the 'performance of the sensor.[86]

4. MXene-based electrochemical sensors for monitoring environmental pollutants

This section is dedicated to exploring the application of electrochemical sensors incorporating MXene materials for the detection and quantification of heavy metal ions, pharmaceutical compounds, synthetic phenolic compounds, and pesticides. The discussion encompasses the fabrication, electrochemical responses, and practical applications of these sensors. The main emphasis in this review is the enhanced electrochemical properties, including factors such as the limit of detection (LOD), detection range, sensitivity, and stability, for each developed sensor. For a comprehensive overview, Table 1 provides a summary of MXene-based electrochemical sensors utilized in the detection of various environmental pollutant species in real samples.

4.1. MXene-based electrochemical sensors designed for the detection of heavy metal ions

The release of heavy metal ions into water bodies, originating from various industrial activities, can result in significant environmental pollution. Furthermore, the contamination of drinking water sources with heavy metal ions poses a severe threat to human health.[8] Therefore, it is of extreme importance to effectively detect toxic heavy metal ions in aqueous media. Dong *et al.*[87] prepared a novel MXene@rGO nanocomposite aerogel-doped UiO-66-NH_2 through a facile and cost-effective method. The successful preparation of the nanocomposite material was confirmed using various advanced analytical techniques, which revealed information regarding the surface morphology and elemental composition. The prepared nanocomposite material was deposited on the surface of a glassy carbon electrode to fabricate an electrochemical sensor for the simultaneous determination of cadmium (Cd^{2+}) and lead (Pb^{2+}) ions, as shown in Fig. 3. The developed UiO-66-NH_2-MXene@rGO/GCE sensor showed an excellent limit of detection 0.46 ppb and 0.40 ppb towards Cd^{2+} and Pb^{2+} ions, respectively. The selective and sensitive determination of both ions was facilitated by the distinctive three-dimensional (3D) network structure of the MXene@rGO composite aerogel. This structure not only enhanced the conductivity of the sensing electrode but also provided a porous framework, allowing increased space for the growth of UiO-66-NH_2. The abundance of amino functional groups within UiO-66-NH_2 served as binding sites for heavy metal ions, facilitating their concentration and enrichment on the sensing surface. Furthermore, the developed sensor demonstrated exceptional resistance to interference, stability, and reproducibility. The practical applications of the sensor were demonstrated with good percentage recoveries from drain and water samples.

Yao *et al.* fabricated a novel heterostructure $BiFeO_3/Ti_3C_2$ MXene ($BiFeO_3$/MXene) composite material *via* the hydrothermal method. Its surface morphology, elemental composition and crystalline nature were confirmed *via* using

Table 1 Electrochemical sensing of different pollutants using MXene-based nanocomposite materials

S. no.	MXene-based modified electrode	Technique	Analyte	LDR	LOD	Ref.
1	UiO-66-NH_2-MXene@rGO/GCE	DPV	Cd^{2+}	—	0.46 ppb	87
			Pb^{2+}		0.40 ppb	
2	$BiFeO_3/Ti_3C_2$/GCE	DPV	Pb^{2+}	—	0.0001 μg L^{-1}	88
3	$Ti_3C_2T_x$ MNR@Au	DPV	Hg^{2+}	0.4 nM–2 μM	17.0 pM	89
4	Ti_3C_2/Fe_3O_4/g-C_3N_4	DPASV	Zn^{2+}	0.26 nM	0.5–0.005 μM	90
			Cd^{2+}	0.21 nM		
			Pb^{2+}	0.10 nM		
			Cu^{2+}	0.11 nM		
			Hg^{2+}	0.12 nM		
5	PANI-Ti_3C_2/GCE	DPV	Hg^{2+}	0.1–20 μg L^{-1}	0.017 μg L^{-1}	91
6	Fe-MOF/MXene/GCE	SWASV	As^{3+}	1–10 ng L^{-1}	0.58 ng L^{-1}	92
7	$Ti_3C_2T_x$/GCE	—	Cd^{2+}	0.50–90 μg L^{-1}	5.0 μg L^{-1}	93
			Pb^{2+}	10–120 μg L^{-1}		
8	CoPB-MXene/GCE	SWASV	Pb^{2+}	1–200 nM	0.97 nM	94
9	$Nb_4C_3T_x$/GEC	SWASV	Pb^{2+}	0–0.5 μM	12 nM	95
10	BiNPs@$Ti_3C_2T_x$/GCE	SWASV	Pb^{2+}	0.06–0.6 μM	10.8 nM	96
			Cd^{2+}	0.08–0.8 μM	12.4 nM	
11	alk-Ti_3C_2/GCE	SWASV	Cd^{2+}	0.1–1.0 μM	0.098 μM	97
			Pb^{2+}	0.1–0.55 μM	0.041 μM	
			Cu^{2+}	0.1–1.4 μM	0.032 μM	
			Hg^{2+}	1–1.9 μM	0.130 μM	
12	3D MGMA/SPCE	DPASV	Zn^{2+}	3–900 μg L^{-1}	0.48 μg L^{-1}	98
			Cd^{2+}		0.45 μg L^{-1}	
			Pb^{2+}		0.29 μg L^{-1}	
13	MXA-CuO/CC	DPASV	Cd^{2+}	4 μg L^{-1} to 800 μg L^{-1}	0.3 μg L^{-1}	99
			Pb^{2+}	4 μg L^{-1} to 1200 μg L^{-1}	0.2 μg L^{-1}	
14	Ti_3C_2-MXene@N-doped carbon/GCE	SWASV	Cd^{2+}	0.1–4.0 μM	2.55 nM	100
			Pb^{2+}	0.05–2 μM	1.10 nM	
15	Bi@d-Ti_3C_2/GCE	DPV	Pb^{2+}	1–20 μg L^{-1}	0.2 μg L^{-1}	101
			Cd^{2+}		0.4 μg L^{-1}	
			Zn^{2+}		0.5 μg L^{-1}	
16	AChE/Ag@$Ti_3C_2T_x$/GCE	DPV	Malathion	10^{-14} to 10^{-8} M	3.27×10^{-15} M	106
17	$Ti_3C_2T_x$-TiO_2/GCE	DPASV	Thiabendazole	0.3–100.0 nM	0.1 nM	107
18	MXene/CNHs/β-CD-MOFs/GCE	DPV	Carbendazim	3.0 nM–10.0 μM	1.0 nM	108
19	MXene@AgNCs/NH_2-MWCNTs/GCE	DPV	Carbendazim	0.3 nM–10 M	0.1 nM	109
20	NF/AChE/$CuCo_2S_4$/CuS/Ti_3C_2 MXene/GCE	DPV	Chlorpyrifos	2.852×10^{-12} to 2.852×10^{-6} M	0.1 pM	110
21	Cu_xO-MWCNTs-COOH/MXene/GCE	DPV	Benomyl	10.0 nM–10.0 M	3.0 nM	111
22	SPE/MXene/Au–Pd/GA/AChE	DPV	Paraoxon	0.1–1000 μgL^{-1}	1.75 μgL^{-1}	112
23	PB@$Ti_3C_2T_x$/GCE	DPV	Malathion	0.0001–1.0 nM	1.3×10^{-5} nM	113
24	$Ti_3C_2T_x$/GCE	DPV	Methiocarb	—	0.19 g mL^{-1}	114
			Diethofencarb		0.46 g mL^{-1}	
25	$MnO_2/Mn_3O_4/Ti_3C_2$/GCE	DPV	Methamidophos	10^{12} to 10^{6} M	1.3^4 to 10^{13} M	115
26	SnO_2/Nb_2CT_x/GCE	DPV	Chlorpyrifos	5.1×10^{-14} to 5.1×10^{-7} M	5.1×10^{-14} M	116
27	MXene/AuPt/AChE-CS/GCE	DPV	Chlorpyrifos	10^{-8}–10^{-3} mg mL^{-1}	1.55 pg mL^{-1}	117
28	TiO_2@MXene/GCE	DPV	Imidacloprid	0.07–10.0 μM	23.3 nM	118
				10.0–70.0 μM		

Table 1 (*Contd.*)

S. no.	MXene-based modified electrode	Technique	Analyte	LDR	LOD	Ref.
29	MXene@Co/NC/GCE	DPV	Carbendazim	0.01–45.0 μM	3.3 nM	119
30	Ag-TiO_2/MXene/GCE	DPV	Paraquat	0.05–1 μM 1–15 μM	0.01 μM	120
31	Nb_2CT_x/NRGO/GCE	SWV	Fluoxetine	1.0–10 μM 10–100 μM	0.34 μM	123
32	*n*Au@$Ti_3C_2T_x$/PABSA/GCE	DPV	Ofloxacin	5.0×10^{-8} to 5.0×10^{-4} mol L^{-1}	3.7×10^{-8} mol L^{-1}	124
33	p-TC/hGO/GCE	DPV	Nitrofurantoin	0.05–158 μM	1.2 nM	125
34	TiC/RGO/GCE	DPV	Furazolidone	0.01–111 μM	2 nM	126
35	ILs_ZnO@MXene/GCE	DPV	5-Fluorouracil	0.5–100 μM	0.03 μM	127
36	Pd–$Ti_3C_2T_x$–P/GCE	DPV	Nitrofurantoin	1–140 nM	0.01 nM	128
37	Au-PPy/$Ti_3C_2T_x$/GCE	DPV	Nitrofurantoin	6–172 nM	0.26 nM	129
38	VC/g-CN NSs NC/GCE	DPV	Clioquinol	0.3–220 μM	2.2 nM	130
39	TFA@Nb_2CT_x/GCE	Chronoamperometry	Rifampicin	100 pM–1 μM	4.8 pM	131
40	g-C_3N_4/Ti_3C/GCE	Amperometry	Ciprofloxacin	0.4–1000 nM	0.13 nM	132
41	Nb_2CT_x/Zn-Co-NC/GCE	DPV	4-Nitrophenol	1–500 M	0.070 M	137
42	Pt@$Ti_3C_2T_x$/GCE	DPV	Bisphenol A	50 Nm–5 M	32 nM	138
43	D-Ti_3C_2TX/GR/GCE	DPV	*p*-Nitrophenol	1–175 μmol L^{-1}	0.16 μmol L^{-1}	139
44	N-Ti_3C_2/PC/GCE	DPV	4-Aminophenol	1–150 μM	0.059 μM	140
45	$Mo_2Ti_2AlC_3$/MWCNT/GCE	DPV	Bisphenol A	0.01–8.50 M	2.7 nM	141
46	Gr/MXene/GCE	DPV	Bisphenol A	10–180 nM	4.08 nM	142
47	Lac-Au/MXene/GCE	DPV	Catechol	0.05–0.15 mM	0.05 mM	143
48	alk-Ti_3C_2/GCE	DPV	Hydroquinone catechol	0.5–150 M	4.8 nM	144
49	$MnMoO_4$-MXene-GCE	DPV	Hydroquinone catechol	5–65 nM	0.26–0.30 nM	145
50	V_2CT_x@NiCoMn–OH-20/GCE	DPV	Hydroquinone	2–1050 μM	0.559 μM	146

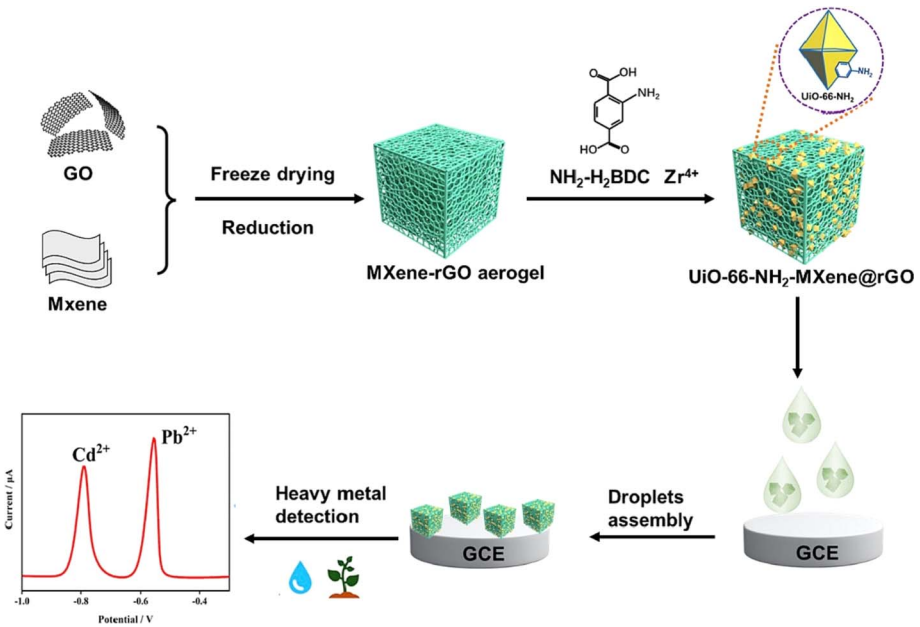

Fig. 3 Synthesis route of UiO-66-NH_2-MXene@rGO/GCE-based modified sensor for the simultaneous determination of Cd^{2+} and Pb^{2+} ions. Reproduced from ref. 87. Copyright (2024), adopted with permission from Elsevier.

sophisticated analytical techniques. Moreover, the fabricated composite material was applied on the surface of a glassy carbon electrode to enhance its conductive nature. The interconnected conductive framework, abundant active sites, and large surface area of the composite material were responsible for the selective and sensitive detection of Pb^{2+} ions. Consequently, the developed sensor showed an outstanding limit of detection of 0.0001 μg L^{-1}. Also, the developed sensor exhibited high sensitivity, good stability, repeatability, reproducibility, no interference from other ions and analytical feasibility to detect Pb^{2+} ions in wastewater.[88] Liu and co-workers synthesized an MXene nanoribbon@gold ($Ti_3C_2T_x$ MNR@Au) composite material through the self-reduction method. The synthesized composite material was characterized using several analytical

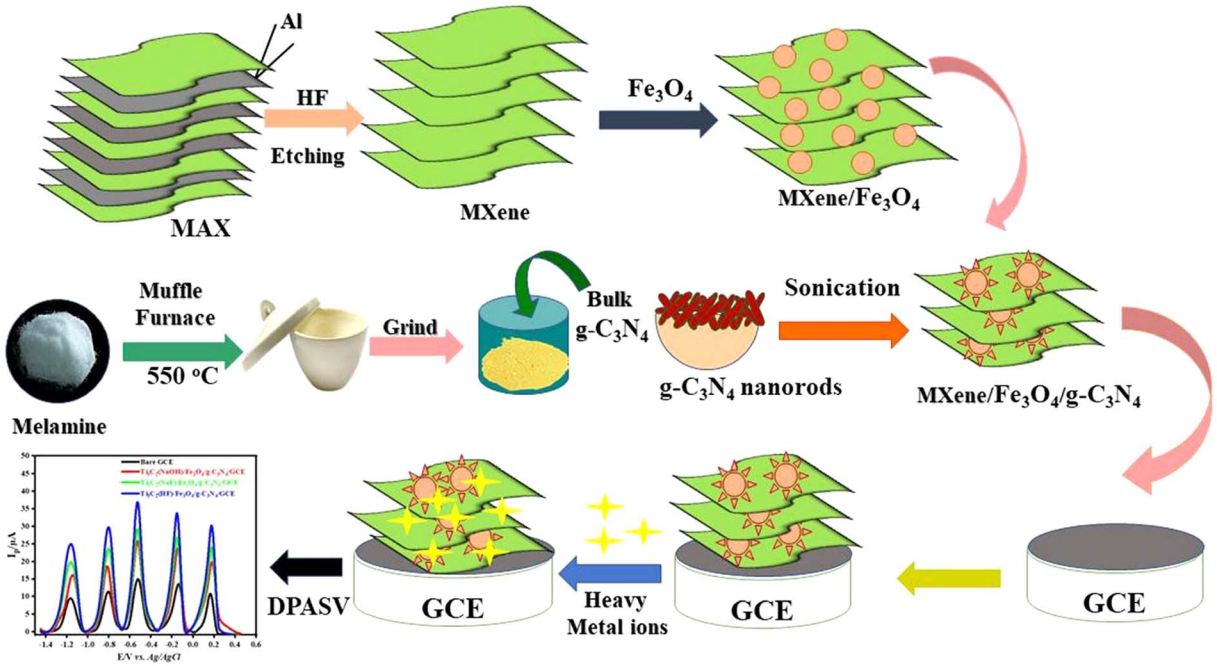

Fig. 4 Synthesis route for Ti_3C_2(HF)/Fe_3O_4/g-C_3N_4 nanocomposite material and detection of Zn^{2+}, Cd^{2+}, Pb^{2+}, Cu^{2+}, and Hg^{2+} ions. Reproduced from ref. 90. Copyright (2023), adopted with permission from Elsevier.

techniques, which provided information about its surface morphology and elemental composition. The as-synthesized composite material was employed for the selective and sensitive detection of Hg^{2+} ions in real samples. The developed sensing strategy exhibited an incredible limit of detection 17.0 pM with a wide linear range of 0.4 nM–2 μM for Hg^{2+} ions. Therefore, this research introduces an innovative composite material and an incorporated tiny system for the highly sensitive, portable, and cost-effective electrochemical monitoring of heavy metal contamination in aqueous environments.[89] Akhtar *et al.* prepared a novel Fe_2O_3 nanochip-loaded MXene/g-C_3N_4 nanocomposite (Ti_3C_2/Fe_3O_4/g-C_3N_4) material through a simple and cost-effective method. The proposed composite material was used for the electrochemical determination of the different heavy metal ions including zinc (Zn^{2+}), cadmium (Cd^{2+}), lead (Pb^{2+}), copper (Cu^{2+}), and mercury (Hg^{2+}) ions in wastewater, as shown in Fig. 4. The proposed electrochemical sensor exhibited an excellent linear response of 0.5 to 0.005 μM with a low limit of detection of 0.26 nM for (Zn^{2+}), 0.21 nM for (Cd^{2+}), 0.10 nM for (Pb^{2+}), 0.11 nM for (Cu^{2+}) and 0.12 nM for (Hg^{2+}) ions in wastewater. The exceptional electroanalytical performance, together with remarkable selectivity and sensitivity, exhibited by the newly developed nanosensor, can be attributed to its heterostructure and coordination facilitated by the combination of MXene and Fe_3O_4/g-C_3N_4. The synergistic effects arising from this combination contributed to enhanced interfacial charge transfer and an increased number of adsorption sites. Furthermore, the efficacy of this sensor was demonstrated through its successful application in detecting metal ions in tap water samples, yielding satisfactory results. This investigation underscores a straightforward methodology for constructing a sensing platform that involves MXene-supported magnetic nanoparticles in conjunction with nitrogen-containing carbon materials, offering an efficient means for the detection of various toxic heavy metal ions in wastewater systems.[90]

Cheng and coworkers engineered a PANI-functionalized Ti_3C_2 nanocomposite material through a facile method. The engineered nanocomposite material was applied for the sensitive and selective electrochemical determination of Hg^{2+} ions in the aquatic environment. Also, the developed electrochemical sensor showed a remarkable wide linear dynamic range of 0.1–20 μg L^{-1} with a low limit of detection of 0.017 μg L^{-1} in the presence of different foreign interferent species. The surface functionalization of Ti_3C_2 with PANI enhanced the electroanalytical properties of the engineered nanocomposite material. Also, the engineered nanocomposite material displayed excellent selectivity, sensitivity, reproducibility, and interferent–resistant properties for the determination of Hg^{2+} ions in the aquatic environment. Given these apparent advantages, the authors anticipated that the proposed method shows potential as a sensitive, selective, and convenient platform for the analysis of real water samples. It also has promising application prospect in the realm of environmental monitoring for the detection different pollutants in real samples.[91] In addition, Xiao and colleagues have prepared an Fe-metal organic framework-decorated MXene (Fe-MOF/MXene) nanocomposite material through a cost-effective and simple hydrothermal method. The prepared nanocomposite material was used for the sensitive electrochemical sensing of arsenic (As^{3+}) ions in an aqueous system, as shown in Fig. 5. Moreover, the proposed electrochemical sensor displayed an exceptional linear response of 1 to 10 ng L^{-1} with a low limit of detection of 0.58 ng L^{-1} As^{3+} ions under the optimized experimental conditions. Additionally, the established sensor demonstrated effective utility in quantifying As^{3+} ions in real water samples, exhibiting notable repeatability and satisfactory recovery rates. Therefore, these outcomes indicate that the synthesized

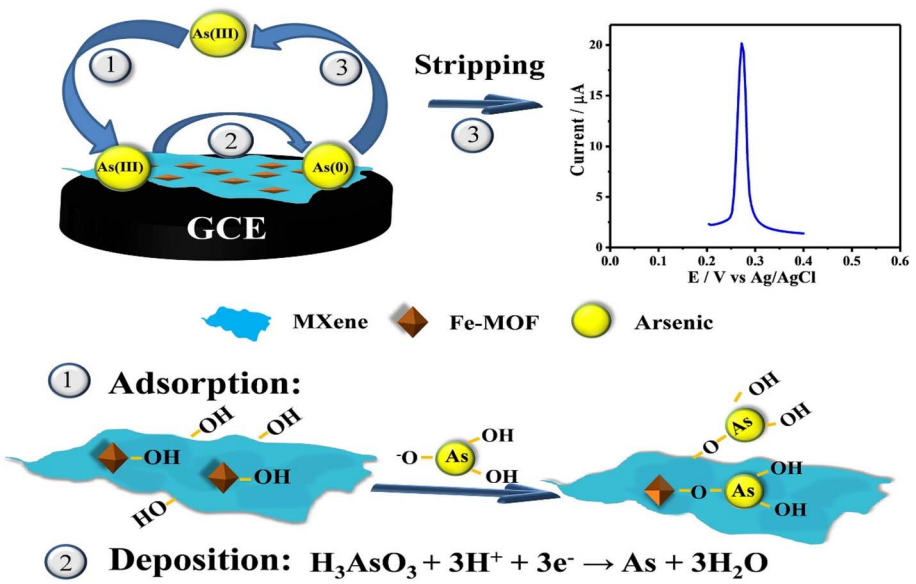

Fig. 5 Adsorption-assisted As^{3+} ion detection on Fe-MOF/MXene/GCE by SWASV. Reproduced from ref. 92. Copyright (2022), adopted with permission from Elsevier.

magnetic nanobiohybrid exhibits extensive potential for application in the detection of various heavy metal ions (HMIs) and other environmental pollutants in the aquatic environment.[92]

Bagheri *et al.* reported the modification of a bifunctional $Ti_3C_2T_x$ MXene through a straightforward condensation reaction, incorporating amine and thiol groups. The fabricated nanocomposite material was applied for the simultaneous detection of Cd^{2+} and Pb^{2+} ions in the aquatic environment. The established electrochemical sensor demonstrated a brilliant wide linear dynamic range of 0.50–90 μg L^{-1} and 10–120 μg L^{-1} with a low limit of detection of 5.0 μg L^{-1} for Cd^{2+} and Pb^{2+} ions, respectively. Therefore, this investigation showcases the applicability of MXenes in the field of analytical chemistry, indicating that progress in developing enhanced methods for the functionalization of MXenes can unlock novel applications for these promising materials.[93] Besides, Guo and coworkers synthesized a 2D $Ti_3C_2T_x$ MXene loading a Co-doped Prussian blue-based nanocomposite material using a simple and cost-effective method. The synthesized nanocomposite material was employed for the determination of Pb^{2+} ions in an aqueous system. The proposed electrochemical sensor presented a wide linear response ranging from 1 to 200 nM with an ultralow limit of detection of 0.97 nM for Pb^{2+} ions under the optimized the conditions. Therefore, the CoPB-MXene-modified glassy carbon electrode (GCE) demonstrated exceptional accuracy when applied to real samples of bottled water, tap water, and lake water. This suggests the promising prospects of the CoPB-MXene-modified GCE for the practical analysis of Pb^{2+} ions. Also, the obtained results in this study suggested that the developed electrochemical sensor can be used for the monitoring of the other pollutants in wastewater.[94] Rasheed *et al.* have prepared an $Nb_4C_3T_x$ (MXene)-based nanocomposite material through a simple method. The developed nanocomposite material was employed for the selective and sensitive detection of Pb^{2+} ions in wastewater, as shown in Fig. 6. The established electrochemical sensor demonstrated a wide linear dynamic response in the range of 0.025 to 0.5 μM, with a low limit of detection of 12 nM for Pb^{2+} ions, even in the presence of various interferent species. These results highlight the suitability of $Nb_4C_3T_x$ as an immobilization platform for the highly sensitive detection of Pb^{2+} ions, offering a broad linear range and a low detection limit. This study marks the inaugural demonstration of the potential application of $Nb_4C_3T_x$ in electrochemical sensing for various environmental pollutants in wastewater systems.[95]

He *et al.* engineered a novel 2D bismuth/MXene ($Bi/Ti_3C_2T_x$) nanocomposite material using a cost-effective and simple method. Due to the preventive influence of the inherent two-dimensional layered structure in $Ti_3C_2T_x$, the Bi nanoparticles exhibited a uniform distribution and secure attachment to the $Ti_3C_2T_x$ substrate. The engineered nanocomposite material was applied for the simultaneous electrochemical detection of Pb^{2+} and Cd^{2+} heavy metal ions in an aquatic system. Moreover, the proposed electrochemical sensor demonstrated a unique linear response ranging from 0.06 to 0.6 and 0.08 to 0.8 μM with an ultralow detection limit of 10.8 nM for Pb^{2+} and 12.4 nM for Cd^{2+} ions, respectively. The potential of $BiNPs@Ti_3C_2T_x$ for the detection of heavy metal ions is attributed to its substantial surface area, rapid electron-transfer capability, environmentally friendly nature, and facile preparation.[96] Furthermore, Zhu *et al.* prepared a 2D accordion-like alk-Ti_3C_2-based nanocomposite material using a simple and cost-effective method. The prepared nanocomposite material was employed for the electrochemical determination of different heavy metal ions including Cd^{2+}, Pb^{2+}, Cu^{2+} and Hg^{2+} in water bodies. The prepared nanocomposite material exhibited a wide linear response ranging from 0.1 to 1.0 μM, 0.1 to 0.55 μM, 0.1 to 1.4 μM and 1 to 1.9 μM with an ultralow detection limit of 0.098 μM, 0.041 μM, 0.032 μM and 0.130 μM for Cd^{2+}, Pb^{2+}, Cu^{2+} and Hg^{2+}, respectively. Therefore, this investigation suggests that

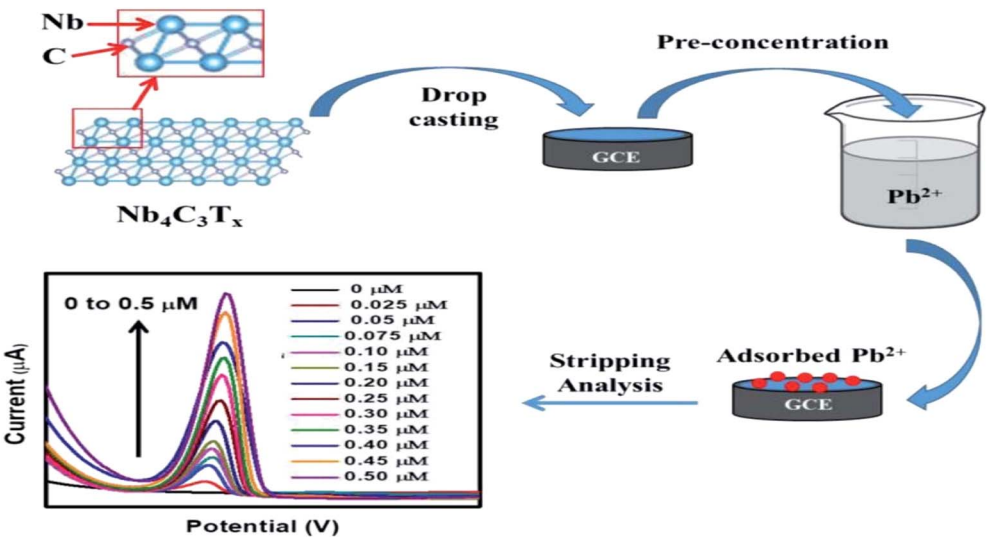

Fig. 6 Synthesis route of $Nb_4C_3T_x$/GEC-modified electrode for the detection of Pb^{2+} ions. Reproduced from ref. 95. Copyright (2020), adopted with permission from The Royal Chemical Society.

functional 2D-MXene materials exhibit promise as a viable platform for the rapid and convenient monitoring of trace concentrations of heavy metal ions in environmental applications.[97] Chen and coworkers fabricated a 3D porous melamine-doped rGO/MXene nanocomposite material using a facile method for the monitoring of three heavy metal ions including Zn^{2+}, Cd^{2+}, and Pb^{2+} ions in wastewater. The proposed electrochemical sensor showed an excellent linear range of 3–900 μg L^{-1} with a low limit of detection of 0.48 μg L^{-1}, 0.45 μg L^{-1} and 0.29 μg L^{-1} for Zn^{2+}, Cd^{2+}, and Pb^{2+} ions, respectively. Significantly, the interconnected 3D architecture formed by the amalgamation of 2D MXene and rGO sheets offered a heightened surface area-to-volume ratio and augmented functional clusters. These attributes were advantageous in enhancing the electrical conductivity and facilitating the absorption of heavy metal ions. Thus, the collective characteristics observed in the fabricated 3D porous MGMA/SPCE electrochemical sensors underscore their significant potential for utilization in monitoring environmental pollution.[98] Wen *et al.* synthesized a novel MXene aerogel-CuO/carbon cloth (MXA-CuO/CC)-based nanocomposite material through a simple and cost-effective method. The prepared nanocomposite material was applied on the surface of a glassy carbon electrode for modification. The modified electrode was applied for the selective and sensitive detection of Cd^{2+} and Pb^{2+} ions in the aquatic environment. The developed sensing electrode exhibited outstanding detection capabilities, demonstrating the simultaneous detection of Cd^{2+} (4 μg L^{-1} to 800 μg L^{-1}) and Pb^{2+} (4 μg L^{-1} to 1200 μg L^{-1}) with detection limits of 0.3 μg L^{-1} (Cd^{2+}) and 0.2 μg L^{-1} (Pb^{2+}) ions in the presence of different interferent species, respectively. Furthermore, the developed composite is likely to offer a versatile electrochemical sensing platform, showing considerable promise for applications in environmental monitoring.[99]

Besides, Zhang and colleagues engineered a 2D Ti_3C_2-MXene@N-doped carbon heterostructure-based nanocomposite material through a facile method. The engineered nanocomposite material was used for the sensitive determination of Cd^{2+} and Pb^{2+} ions in the aqueous environment. The sensor exhibited a unique performance with an ultra-low detection limit of 2.55 nM for Cd^{2+} and 1.10 nM for Pb^{2+} ions in the presence of different foreign interferent species, respectively. The heterostructure formed by N–C and Ti_3C_2-MXene enhanced the conductivity of the composites by expediting electron transfer. The nitrogen-doping in Ti_3C_2@N–C introduced adsorbent sites for electrons to coordinate with heavy metal ions (HMIs). The presence of the heterostructure and nitrogen-coordinated coordination enhanced the interface charge transfer and augmented the number of selective adsorption sites. This improvement contributed to the enhanced performance in determining metal concentrations. Therefore, this investigation introduces a novel approach aimed at enhancing the electrochemical properties of Ti_3C_2-MXene through the incorporation of a heterostructure and the nitrogen-doping effect. Consequently, a highly sensitive sensor was developed for the selective and simultaneous determination of heavy metal ions (HMIs) and other environmental pollutants in water bodies.[100] Zhu and coworkers prepared a novel 2D MXene-bismuth (Bi@d-Ti_3C_2) nanocomposite material using a simple and cost-effective method. The prepared nanocomposite material was employed to determine Pb^{2+}, Cd^{2+} and Zn^{2+} ions in the aquatic environment. The proposed electrochemical sensor showed an excellent linear response of 1 to 20 μg L^{-1} with a low limit of detection of 0.2, 0.4 and 0.5 μg L^{-1} for Pb^{2+}, Cd^{2+} and Zn^{2+} ions, respectively. Therefore, the obtained results in this study suggested that the developed electrochemical sensor can be applied for the determination of other environmental pollutants in wastewater.[101]

4.2 MXene-based electrochemical sensor designed for the detection of pesticides

The escalating demand for food and agricultural resources underscores the necessity of employing pesticides to safeguard plants. However, this strategy concurrently presents risks of pesticide poisoning and environmental hazards.[102] Pesticides play a crucial role in safeguarding agricultural crops against insects, weeds, and diseases.[103] However, a notable portion of these pesticides does not reach their intended targets, resulting in unintended consequences such as soil contamination and pollution of ground and surface water resources. Additionally, the unregulated and excessive use of pesticides has raised concerns regarding food contamination and environmental pollution, especially in aquatic and agricultural settings. Residues of pesticides have been identified in various sources such as vegetables, fruits, processed foods, air, soil, and water, potentially serving as an entry point into the food chain. Dietary exposure to agricultural pesticides presents a significant public health risk, particularly in developing nations, having potential immediate and long-term consequences on human health.[104,105] Chemical pesticides can adversely impact human health by exhibiting cytotoxic, carcinogenic, and mutagenic properties. Scientists have predominantly utilized traditional methodologies including gas chromatography-tandem mass spectrometry (GC-MS), high-performance liquid chromatography (HPLC), immunoassays, and colorimetry for the qualitative and quantitative assessment of pesticides in aqueous media. However, although these techniques are effective, rapid, and widely adaptable, they are impractical for regular organophosphate (OP) residue analysis. Their limitations include significant equipment costs, prolonged analysis durations, lack of portability, reliance on skilled personnel, and complex preprocessing requirements. Furthermore, the detection limits of these methods typically surpass the actual concentrations of analytes in samples. Table 1 delineates the performance metrics associated with the detection of pesticides in aqueous media utilizing MXene-based electrochemical sensors. Jiang and colleagues fabricated a novel 2D Ag@$Ti_3C_2T_x$-functionalized nanocomposite material through a simple method, which was used for the selective detection of organophosphate malathion pesticide (OP) in real simples, as displayed in Fig. 7. The developed electrochemical sensor exhibited an exceptional linear response in the concentration range of 10^{-14} to 10^{-8} M, with a low limit of detection of 3.27×10^{-15} M for malathion

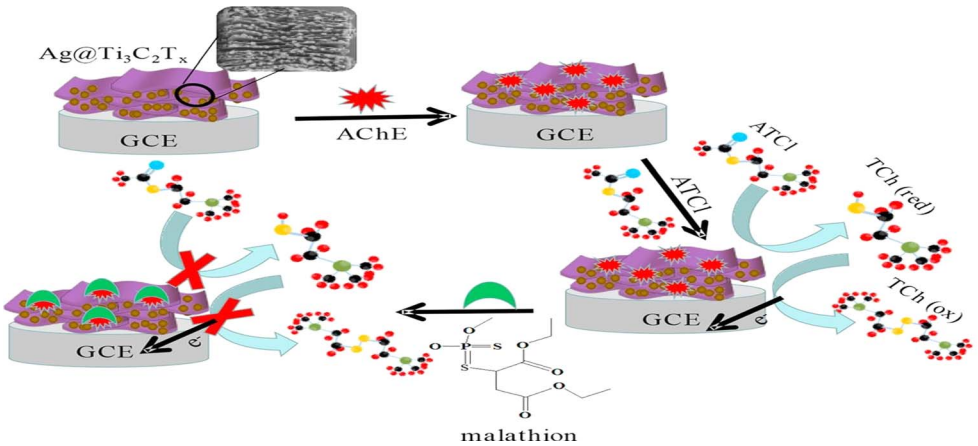

Fig. 7 Synthesis route of Ag@$Ti_3C_2T_x$ for the detection of the organophosphate pesticide malathion. Reproduced from ref. 106. Copyright (2018), adopted with permission from Elsevier.

pesticide. Due to the remarkable characteristics of the Ag@$Ti_3C_2T_x$ nanocomposite material, it exhibited a high degree of linearity characterized by a low detection limit. This sensor exhibited outstanding sensitivity, acceptable stability, rapid electrochemical response, and reliable reproducibility. Therefore, this investigation expanded the utilization of MXenes within the realm of sensors, opening up diverse opportunities for the advancement of electrochemical sensors based on MXenes for applications in environmental monitoring in real samples.[106]

Zhong *et al.* created an electrode made of a hetero-structured $Ti_3C_2T_x$-TiO_2 composite, which could detect thiabendazole (TBZ). This sensor exhibited a linear range of 0.3 to 100.0 nM and a limit of detection (LOD) of 0.1 nM, according to the anodic stripping peak signal change of Cu^{2+} in the media. In fruit and water samples, this sensor demonstrated outstanding anti-interference, repeatability, stability, and applicability. This highlights its prospective utility in meeting the demands of environmental monitoring and ensuring food safety.[107] Similarly, Tu *et al.* prepared an MXene/carbon nanohorn/β-cyclodextrin-metal–organic framework (MXene/CNHs/β-CD-MOFs) composite material using a simple and cost-effective method. The prepared nanocomposite material was utilized for the electrochemical monitoring of carbendazim (CBZ) pesticide in wastewater. The established electrochemical sensor revealed good wide linear response 3.0 nM to 10.0 μM with low limit of detection 1.0 nM was observed for carbendazim (CBZ) pesticide. Additionally, the fabricated sensor exhibited notable selectivity, reproducibility, and enduring stability, demonstrating satisfactory suitability for analysis in real samples. This study underscores the significant promise of the developed method for analytical applications in the monitoring of various pollutants in real matrices.[108] Zhong and coworkers engineered an MXene@Ag-based ratiometric based nanocomposite material by utilizing a facile method, which was applied for the electrochemical monitoring of carbendazim (CBZ) pesticide in a real matrix. The developed sensor had an LOD of 0.1 nM and linear range of 0.3 nM to 10 M. Moreover, in vegetable samples, the sensor exhibited high selectivity, excellent reproducibility, long-term stability, and satisfactory applicability. These results suggest the potential suitability of this sensor for environmental monitoring and meeting food safety.[109] Mi *et al.* synthesized a novel 2D $CuCo_2S_4$/CuS/Ti_3C_2 heterostructure nanocomposite material through a simple and cost-effective method. Also, the developed nanocomposite material was employed for the electrochemical determination of chlorpyrifos pesticide in real samples, even in the presence of various foreign interferent species. The established electrochemical sensor showed a remarkable wide linear response of 2.852×10^{-12} to 2.852×10^{-6} with a low limit of detection of 0.1 pM for chlorpyrifos pesticide, as shown in Fig. 8(a and b). Also, the developed electrochemical sensor exhibited exceptional selectivity, excellent reproducibility, stability, and acceptable applicability for the detection of chlorpyrifos pesticide, as shown in Fig. 8(c). The viability of this approach was validated through the quantification of chlorpyrifos pesticide in wastewater samples, yielding a satisfactory recovery. In summary, the nano-$CuCo_2S_4$/CuS/Ti_3C_2/MXene composite has emerged as a promising material candidate for application in electrochemical sensors designed for detecting chlorpyrifos pesticide in wastewater systems.[110]

Zhong *et al.* prepared a 3D nano-Cu_xO-MWCNT-COOH/MXene-based heterostructure nanocomposite material using a simple method. The hierarchical nano-CuO-decorated MWCNT-COOH/MXene composite-based material was employed as a highly sensitive and selective electrochemical sensor for the detection of benomyl (BN) in real samples. This sensor exhibited an LOD of 3.0 nM and a linear range of 10.0 nM to 10.0 M. It was also successfully applied in apple samples, showing excellent long-term stability and repeatability. Due to these properties, the developed electrochemical sensor can be utilized for the detection of environmental pollutants in real samples.[111] Zhao *et al.* and colleagues synthesized an MXene/Au–Pd nanocomposite using a facile strategy and employed it as a highly efficient electrochemical sensor for detecting paraoxon pesticide in agricultural products. The established biosensor

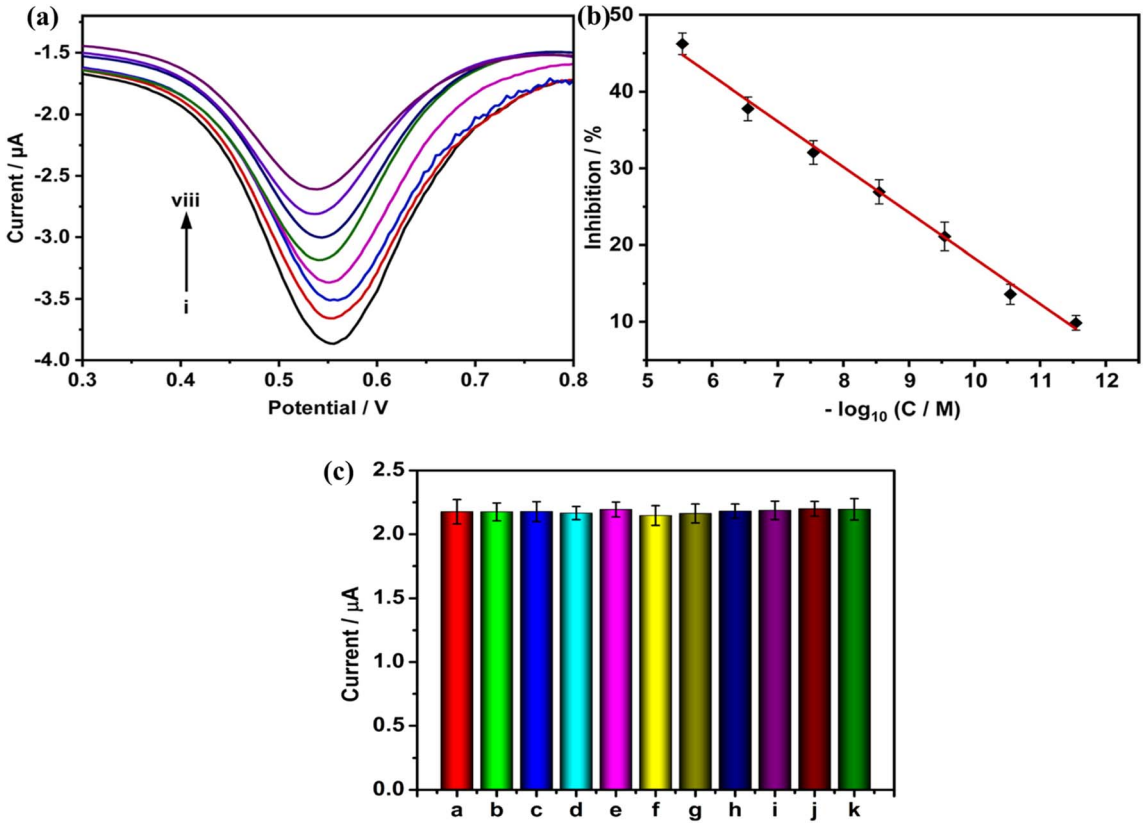

Fig. 8 (a and b) DPV responses of the modified electrode and (c) effect of foreign interferent species in the determination of chlorpyrifos pesticide. Reproduced from ref. 110. Copyright (2022), adopted with permission from Elsevier.

exhibited a broad linear response to paraoxon pesticide, ranging from 0.1 to 1000 μgL^{-1}, and boasted a minimal detection limit of 1.75 μg L^{-1}. Additionally, when paraoxon was utilized as a representative pesticide, the developed sensor showcased an extensive linear detection range, low detection limit, remarkable sensitivity, and practical usability for real-world samples. This suggests that the use of ultrathin MXene nanosheets can expand their application as electrochemical sensors in the analysis of environmental contaminants.[112] Additionally, He and colleagues designed a Prussian blue (PB)–$Ti_3C_2T_x$ hybrid composite (PB@$Ti_3C_2T_x$)-modified glassy carbon electrode (GCE) for the determination of malathion pesticide in real matrices. The developed electrochemical sensor exhibited a wide linear dynamic range of 0.0001–1.0 nM with a low limit of detection of 1.3 × 10^{-5} nM for malathion pesticide. Furthermore, the suggested approach was effectively employed for the quantification of malathion pesticide in real samples, yielding satisfactory outcomes. PB@$Ti_3C_2T_x$/GCE exhibited commendable reproducibility and stability, coupled with superior catalytic activity and resistance against interference species.[113] In another study, methiocarb, diethofencarb, and carbamate pesticides were quickly screened using an electroanalytical method. The authors employed colloidal single/few layer $Ti_3C_2T_x$ MXene flakes prepared using the minimally intensive layer delamination (MILD) method. This sensor showed acceptable recoveries in actual samples and a detection limit of 0.19 g mL^{-1} for methiocarb and 0.46 g mL^{-1} for diethofencarb. Consequently, the modified electrode utilizing $Ti_3C_2T_x$ flakes was applied for the simultaneous electrochemical screening of carbamate pesticides, specifically methiocarb and diethofencarb. This electrode exhibited remarkable conductivity, electronic properties, and hydrophilic characteristics. The sensor design incorporating $Ti_3C_2T_x$ flakes highlighted its effective potential in various applications related to electrochemical sensing, biosensing, and wearable devices.[114] Song *et al.* developed MnO_2/Mn_3O_4 and Ti_3C_2 MXene/Au NP composites derived from MOFs to create a novel electrochemical sensing platform for the detection of organophosphorus pesticides (OPs). The combination of MXene/Au NPs with the three-dimensional (3D) MnO_2/Mn_3O_4 hierarchical microcuboids formed from Mn-MOF produced an excellent electrochemical performance, good environmental biocompatibility, and synergistic signal amplification effect. The AChE-Chit/MXene/AuNPs/MnO_2/Mn_3O_4/GCE sensing platform could identify methamidophos in the concentration range of 10^{12} to 10^{6} M with a low limit of detection (1.3^{4} to 10^{13} M). With excellent recoveries (95.2–101.3%), this biosensor was effectively used to detect methamidophos in real samples. The distinctive structures and exceptional properties exhibited by these composites make them appealing materials for diverse electrochemical sensors, capable of monitoring not only pesticide residues but also other environmentally harmful

chemicals.[115] Besides, Guo and colleagues fabricated a novel SnO_2/Nb_2CT_x MXene nanocomposite material through a simple method, which was used for the sensitive determination of chlorpyrifos pesticides in the aquatic environment. The proposed electrochemical sensor showed an excellent linear response 5.1×10^{-14} to 5.1×10^{-7} M with a low limit of detection of 5.1×10^{-14} M for chlorpyrifos pesticide. Certainly, the highly conductive Nb_2CT_x MXene, operating as a substrate material, played a crucial role in preventing the agglomeration of nanoparticles (NPs) and promoting swift electron migration. This can be ascribed to the confinement effect and the well-known accordion-like layered structure of the MXene. Additionally, SnO_2 attached on both sides of the Nb_2CT_x MXene nanosheets contributed to the significant surface area, abundant surface groups, and active sites. These features collectively retained a substantial number of electrons at the interface of the heterojunction. Therefore, the results obtained in this study suggest that the developed electrochemical sensor can be applied for the determination of various other environmental pollutants in wastewater systems.[116] Ding *et al.* fabricated a novel MXene/AuPt/AChE-CS nanocomposite material using a simple and cost-effective method. The developed nanocomposite material was applied for the electrochemical detection of chlorpyrifos pesticide in wastewater. The proposed sensor exhibited an excellent linear response of 10^{-8} to 10^{-3} mg mL^{-1} and limit of detection of 1.55 pg mL^{-1} for chlorpyrifos pesticide in the presence of different interferent species. The developed sensor synergistically harnessed the distinctive electrocatalytic properties of MXene nanosheets and the synergistic effects of AuPt bimetallic nanoparticles. This combination not only enhanced the electron transfer capabilities but also augmented the electroactive surface area, facilitating the immobilization of acetylcholinesterase (AChE). Moreover, the electrochemical sensor prepared in this study demonstrated notable sensitivity, satisfactory repeatability, and outstanding stability. These outcomes suggest its significant potential for the detection of organophosphorus pesticides in wastewater systems.[117] Furthermore, Deng *et al.* constructed a hetero-structured TiO_2@MXene-based nanocomposite material through a simple method. The prepared nanocomposite material was deposited on the surface of a glassy carbon electrode to create a modified electrode for the selective and sensitive detection of imidacloprid pesticide. Also, the created modified electrode displayed a remarkable wide linear dynamic range of 0.07–10.0 μM and 10.0–70.0 μM with a low limit of detection of 23.3 nM for imidacloprid pesticide in the presence of different interferent species. The material design involved the initial growth of TiO_2 nanoparticles directly on MXene, serving as a scaffold to prevent the stacking of the MXene nanosheets. This resulted in the creation of a well-defined TiO_2@MXene heterostructure, exhibiting a notable layered configuration and a substantial specific surface area. Subsequent treatment using electrochemical activation significantly augmented the presence of surface oxygen vacancies (VOs) within the TiO_2@MXene composite. This enhancement notably boosted its conductivity and adsorption capabilities, which was attributed to the increased concentration of VOs.[118] Similarly, Chen *et al.* prepared a novel 2D ZIF-67-derived Co and N-doped carbon (Co/NC) particle-modified multilayer MXene (MXene@Co/NC)-based composite material using a simple method for the electrochemical detection of carbendazim pesticide in the aquatic environment. The established electrochemical sensor presented an exceptional wide linear response ranging from 0.01 μM to 45.0 μM with low a limit of detection of 3.3 nM for carbendazim pesticide under the optimized experimental conditions. Additionally, the presented sensor exhibited outstanding resistance to interference, superior reproducibility, and remarkable stability. Thus, its practical application for detecting carbamazepine pesticide was successfully demonstrated in a lettuce sample, emphasizes the potential of MXene@Co/NC as a promising material for fabricating electrochemical sensors for pesticides in aquatic systems.[119] Hou and colleagues have fabricated a 2D Ag–TiO_2/MXene composite material through a facile approach and used it for the electrochemical detection of paraquat (PQ) pesticide using the differential pulse voltammetry (DPV) mode. The proposed electrochemical sensor demonstrated a remarkable concentration response from 0.05 to 1 μM and 1 μM to 15 μM with a low limit of detection of 0.01 μM paraquat pesticide. The remarkable capability of the Ag–TiO_2/MXene electrode material for detecting paraquat can be ascribed to the synergistic effect achieved through the incorporation of Ag and TiO_2 in MXene. In summary, the surface modification of MXenes *via* functionalization presents a viable approach for constructing electrochemical sensors with ultra-sensitive characteristics.[120]

4.3 MXene-based electrochemical sensor designated for the detection of antibiotic drugs

Antibiotics encompass a diverse group of compounds, including natural, synthetic, and semi-synthetic substances capable of either killing or inhibiting the growth of bacteria, archaea, viruses, protozoa, microalgae, and fungi. The classification of antibiotics is based on their chemical structure or mechanism of action, resulting in distinct classes such as β-lactams, quinolones, tetracyclines, and macrolides.[121] Nevertheless, the majority of antibiotics consumed by both humans and animals are excreted in the form of either unchanged drugs or metabolites. Consequently, the primary route of antibiotic discharge into the environment occurs through the excreta of humans and livestock, as well as through pharmaceuticals used in the aquaculture industry and the wastewater generated during production processes.[122] Therefore, it urgent to develop sensitive and simple methods for the monitoring of the antibiotic waste in environmental samples. Table 1 displays the MXene-based electrochemical modified sensors for the detection of different antibiotics drugs in real matrices. Similarly, Chen and coworkers prepared the Nb_2CT_x/NRGO nanocomposite material through a facile approach and utilized it for the electrochemical monitoring of fluoxetine antibiotic drug in wastewater. The proposed electrochemical sensor demonstrated an exceptional linear response ranging from 1.0–10 μM and 10–100 μM with a low limit of detection of 0.34 μM for fluoxetine pesticide under the optimized experimental

conditions. Furthermore, this sensor demonstrated commendable selectivity, repeatability, reproducibility, and stability. It exhibited the capacity to sensitively detect FLX (fluoxetine) in clinical biological fluids, specifically in human serum and urine samples.[123] In addition, Yang engineered a gold nanoparticle (*n*Au)@MXene ($Ti_3C_2T_x$)/poly-*p*-aminobenzene sulfonic acid (PABSA)-based composite material through a cost-effective and simple method. The engineered nanocomposite material was deposited on the surface of a glassy carbon electrode for modification and enhanced the conductivity of the glassy carbon electrode for the selective sensing of ofloxacin antibiotic drug in real samples. The created electrochemical sensor exhibited a good linear response ranging from 5.0×10^{-8} to 5.0×10^{-4} mol L^{-1} with a low limit of detection of 3.7×10^{-8} mol L^{-1} for ofloxacin antibiotic drug. The electrode composed of nAu@$i_3C_2T_x$/PABSA/GCE exhibited favorable selectivity, together with notable repeatability and reproducibility. Also, the proposed electrochemical sensor displayed good percent recoveries of ofloxacin antibiotic drug from commercial samples, which highlight its excellent sensing capability. Considering these findings, the current study illustrates the formulation of functional electrocatalysts, providing a foundation for the exploration and creation of sustainable electrode materials conducive to simultaneous electrochemical detection.[124] Besides, Devi *et al.* fabricated a novel 2D functional nanocomposite of holey-graphene oxide with partially-oxidized MXene titanium carbide (p-TC/hGO) material through a simple method and utilized it for the electrochemical sensing of nitrofurantoin antibiotic drug in a real matrix. The developed electrochemical sensor displayed an outstanding wide linear dynamic range of 0.05 to 158 μM with a low limit of detection of 1.2 nM for the nitrofurantoin antibiotic drug. The hGO nanosheets constructed a three-dimensional network, enhancing the electron transport by establishing connections among the p-TC flakes. The composite of p-TC/hGO possessed an expanded surface area, which is primarily attributed to the abundant perforations in the basal plane nanosheets of hGO and the layered arrangement of p-TC featuring oxygen-rich surface functional groups. The electrode, modified with p-TC/hGO, exhibited a significantly enhanced electrocatalytic performance for the detection of nitrofurantoin antibiotic drug. The sensor presented herein showcased the concurrent electrochemical detection of nitrofurantoin antibiotic drug in urine samples. Consequently, it holds promise for potential utilization in the real-time clinical analyses of different antibiotic drugs in environmental samples.[125]

Additionally, Rajakumaran and coworkers prepared a 2D-TiC/RGO nanocomposite material using a cost-effective and facile approach. The established nanocomposite material was used as an electrochemical sensor for the detection of furazolidone antibiotic drug in real samples. The developed electrochemical sensor exhibited the good linear response of 0.01–111 μM and a low limit of detection of 2 nM for furazolidone antibiotic drug in the presence of different interferent species. Additionally, the developed furazolidone sensor was successfully applied for real-time analysis in human serum, as well as in food samples, including cow milk and pork liver, yielding satisfactory recovery outcomes. Therefore, these findings suggest that the composite material synthesized in this study holds promise as a potential candidate for furazolidone sensors in applications related to biology and food.[126] Moreover, Shekh *et al.* constructed a novel IL_ZnO@MXene-based nanocomposite material through a simple method. The constructed nanocomposite material was employed for the electrochemical monitoring of the 5-fluorouracil drug in real matrices, even in the presence of various interfering species. The proposed electrochemical sensor demonstrated an excellent wide linear dynamic range of 0.5–100 μM with a low limit of detection of 0.03 μM. Furthermore, the outcomes substantiate that ionic liquids (ILs) augment the interfacial connectivity between the ZnO nanowires (NWs) and MXene nanosheets *via* electrostatic interactions. This enhancement contributed to an improved rate of charge transfer, heightened sensing capability, and increased signal intensity for the detection of drugs in real samples including biological and wastewater systems.[127] Tumrani *et al.* created a Pd–$Ti_3C_2T_x$–P composite material through a facile method and used it for the electrochemical monitoring of nitrofurantoin antibiotic drug in wastewater. The developed electrochemical sensor demonstrated a remarkable concentration range of 1 to 140 nM with a low limit of detection of 0.01 nM. Moreover, the engineered sensor exhibited exceptional selectivity for nitrofurantoin antibiotic drug, demonstrating resistance against potential interfering substances such as biomolecules, drugs, and metal ions. Significantly, this sensor demonstrated the ability to selectively detect nitrofurantoin antibiotic drug in complex environmental matrices, including hospital waste effluent samples. Therefore, the proposed design provides a straightforward approach for the development of advanced electrocatalytic sensors with potential applications in monitoring emerging pharmaceutical pollutants in real matrices.[128] Similarly, Vilian and colleagues prepared novel nanosized Au nanoparticle-decorated PPy-MXene (Au-PPy/$Ti_3C_2T_x$) using a simple route and deposited it on the surface of a glassy carbon electrode to create a modified electrode for the sensitive and selective determination of nitrofurantoin antibiotic drug in real samples, as shown in Fig. 9(a–c). The proposed electrochemical sensor showed a good linear response of 6 to 172 nM with an ultra-low limit of detection of 0.26 nM for nitrofurantoin antibiotic drug under the optimized experimental conditions. The proposed sensor also exhibited good sensitivity of 6.4121 μA nM^{-1} cm^{-2}, reproducibility, selectivity and ant-interferent activity for nitrofurantoin antibiotic drug. The delineated fabrication methodology offers a viable strategy for producing electrodes suitable for the expeditious on-site assessment of environmentally significant pollutants at low concentrations in wastewater systems.[129]

In another study, Devi *et al.* fabricated a 2D MXene vanadium carbide ($V_8C_7T_x$; VC) nanosheet-encapsulating graphitic carbon nanosheet nanocomposite (VC/g-CN NSs NC) using a facile method. The fabricated nanocomposite material was used for the electrochemical monitoring of the clioquinol antibiotic drug in a real matrix. The established electrochemical sensor displayed an outstanding wide linear dynamic range of 0.3–220 μM with a low limit of detection of 2.2 nM for clioquinol

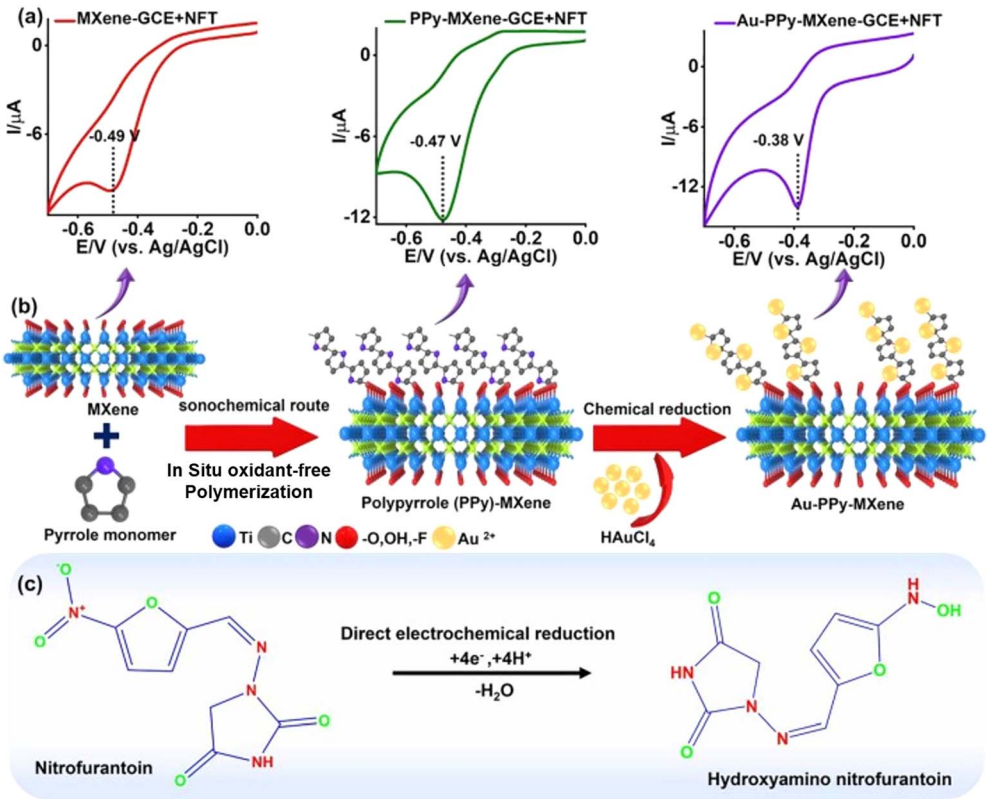

Fig. 9 (a) CV response of different modified electrodes towards nitrofurantoin drug, (b) synthesis route of Au-PPy-MXene nanosheets, and (c) mechanism responsible for the electrocatalytic reduction of NFT on Au-PPy-MXene-GCE. Reproduced from ref. 129. Copyright (2023), adopted with permission from Elsevier.

antibiotic drug, as shown in Fig. 10(a–c). Consequently, VC/g-CN NSs/GCE demonstrated noteworthy electrocatalytic sensing capabilities for clioquinol antibiotic drug, exhibiting exceptional reproducibility, repeatability, and stability. Moreover, the proposed sensor enhanced the electrochemical detection of the clioquinol antibiotic in real-world samples, showcasing its practical significance. The outlined methodology establishes a highly efficient electrochemical electrode for clioquinol antibiotic sensors, paving the path for the prospective exploration of highly active carbide-based carbon nanocomposites in diverse electrochemical contexts.[130]

Besides, Ankitha *et al.* engineered a hierarchical porous highly stable trifluoroacetic acid (TFA)-modified Nb_2CT_x MXene (TFA@Nb_2CT_x) nanocomposite material through a simple and cost-effective method. The incorporation of trifluoroacetic acid as interlayer spacers effectively suppressed the aggregation of MXene flakes, yielding a distinct porous structure. This led to an increased effective surface area, consequently enhancing both electrical conductivity and electrocatalytic activity. The engineered nanocomposite material was employed for the electrochemical sensing of rifampicin antibiotic drug in wastewater. Also, the developed electrochemical sensor presented an exceptional linear response in the range of 100 pM to 1 μM with a low limit of detection of 4.8 pM for rifampicin antibiotic drug. Moreover, owing to its commendable stability and selectivity, the recently engineered sensor was applied for the detection of rifampicin antibiotic drug in real-world samples, yielding satisfactory outcomes.[131] Furthermore, Yuan and coworkers prepared a g-C_3N_4/Ti_3C-based composite material *via* a simple synthesis route and employed it as a selective and sensitive electrochemical sensor for the determination of ciprofloxacin antibiotic drug in real samples. The proposed electrochemical sensor exhibited a good linear response ranging from 0.4 to 1000 nM with a low limit of detection of 0.13 nM for ciprofloxacin antibiotic drug. Furthermore, the developed sensor exhibited prolonged stability, excellent reproducibility, and selectivity. Subsequently, the detection of ciprofloxacin antibiotic drug in actual commercial samples was conducted to validate the practical applicability of the developed sensor. The findings of this investigation illuminate the application of the developed sensor for the detection of different environmental pollutants from wastewater systems.[132]

4.4 MXene-based electrochemical sensors designed for the detection of synthetic phenolic compounds

Synthetic phenolic compounds are compounds that contain one or more hydroxyl groups in benzene and may contain other groups, which are created artificially through chemical synthesis. Synthetic phenolic compounds can be divided into several groups, such as bisphenol, alkylphenols, and halogenated phenols. Moreover, different synthetic phenolic compounds such as bisphenol, aminophenol, catechol,

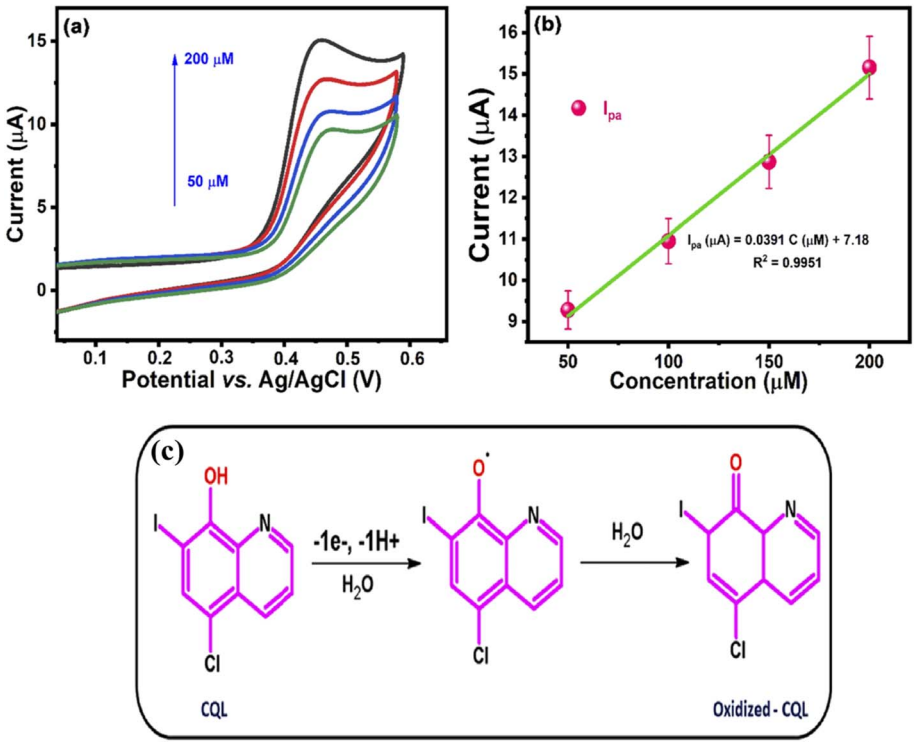

Fig. 10 (a) CVs for varying concentrations of CQL (50–200 μM) over the surface of VC/g-CN NSs/GCE, (b) linear plot of concentration *vs.* current, and (c) electro-oxidation mechanism of clioquinol drug on the surface of VC/g-CN NSs/GCE. Reproduced from ref. 130. Copyright (2023), adopted with permission from Elsevier.

nitrophenol, hydroquinone and 2,4-dichlorophenol are used in polycarbonate plastics, insecticides, cosmetics, food preservatives, *etc.* Due to their excessive use, these synthetic phenolic compounds can cause adverse effects on human health including reproductive issues, developmental delays, hormonal unbalance, kidney damage, liver damage, eye irritation and other serious dangerous diseases.[133–136] Therefore, it is very important to detect these pollutants in wastewater samples. Huan and coworkers suggested a straightforward self-assembly technique to create a novel heterostructure (MXene/ZIF) made of bimetallic Zn, Co embedded N-doped carbon (Zn-Co-NC) nanocages and derived from Zn-Co-ZIFs and Nb_2CT_x. The modified Nb_2CT_x/Zn-Co-NC hybrid electrodes were used to detect 4-nitrophenol (4-NP) electrochemically. According to the SEM images, Zn-Co-NC was successfully inserted to prevent Nb_2CT_x from restacking. The effective synthesis of the bimetallic Zn, Co embedded N-doped carbon nanocage was shown by EDS and XPS. A wide linear range was obtained under ideal circumstances in the range of 1 M to 500 M. A high sensitivity of 4.65 M cm^{-2} and low detection limit of 0.070 M were achieved. Moreover, the Nb_2CT_x/Zn-Co-NC sensor also possessed exceptional selectivity and durability. The distinctive structural attributes and outstanding characteristics of MXenes/ZIFs make them promising candidates as substitute materials in diverse electrochemical sensors for the identification of additional hazardous organic pollutants in wastewater systems.[137] Similarly, Rasheed and colleagues created a nanocomposite of platinum nanoparticles and $Ti_3C_2T_x$ (Pt@$Ti_3C_2T_x$) employing delaminated $Ti_3C_2T_x$ nanosheets. The nanosheets served as both a reducing agent and a conductive scaffold to self-reduce Pt salt to Pt nanoparticles. It was discovered that 10%Pt@$Ti_3C_2T_x$ had the greatest electrochemical activity in the anodic potential window after they characterized the electrochemical activity of Pt@$Ti_3C_2T_x$ nanocomposites with varying Pt loadings. They later developed an electrochemical sensor for the detection of bisphenol A (BPA), a prevalent environmental pollutant, using this nanocomposite, as shown in Fig. 11(a and b). Under ideal circumstances, the oxidation peak of BPA showed a detection limit of 32 nM and was proportionate to the analyte concentration in the range of 50 nM to 5 M, as shown in Fig. 11(c and d). The performance of this sensor was effectively tested using samples of fresh milk and drinking water. Moreover, a feasibility assessment for practical implementation was conducted in the context of industrial wastewater. Based on these findings, the authors confidently asserted that their study paves the way for the development of MXene-based sensors employing Ti_3C_2, Nb_2C, or V_2C, aimed at detecting a spectrum of phenolic and other organic compounds in industrial wastewater.[138]

X. Wang *et al.* developed a sensor for the rapid electrochemical detection of *p*-nitrophenol (*p*-NP), a significant environmental pollutant. The Ti_3C_2TX MXene/graphene composite that served as the sensor foundation was made using a minimally intensive layer delamination (MILD) technique and a self-assembly procedure. SEM, XRD, AFM, and Raman spectroscopy were all used to characterize the final product. The D-Ti_3C_2TX/

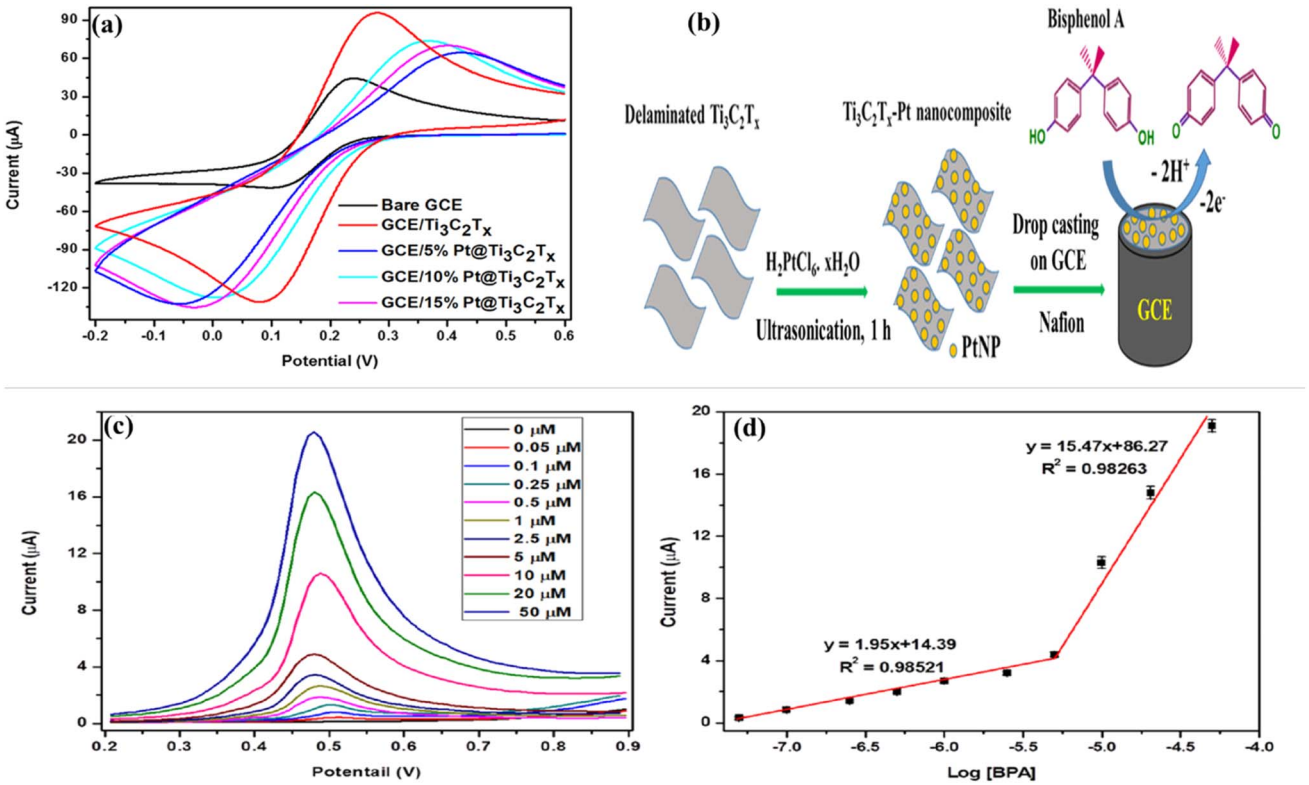

Fig. 11 (a) CV response of different modified electrodes for BPA, (b) electro-oxidation mechanism of BPA, (c) DPV response of BPA, and (d) calibration plot of BPA detection on the surface of the modified electrode. Reproduced from ref. 138. Copyright (2021), adapted with permission from Elsevier.

GR/GCE sensor was made by modifying a glassy carbon electrode (GCE) with the alloy. Chronocoulometry, electrochemical impedance spectroscopy, and cyclic voltammetry were all used to examine the electrochemical behavior of the sensor. Due to the abundance of active sites, quick electron transfer, and good electro-catalytic performance of the D-Ti_3C_2TX/GR composite, the sensor demonstrated a strong electrochemical response to the *p*-NP reduction reaction. Also, the developed sensor exhibited the wide linear dynamic range of 1 to 175 μmol L^{-1} with an ultra-low detection limit of 0.16 μmol L^{-1} for *p*-NP in the aquatic environment. In addition, the investigation involved the assessment of its anti-interference capabilities, reproducibility, stability, and recovery during the analysis of real samples. Therefore, this research introduces an innovative and highly sensitive approach for the swift quantification of *p*-NP in environmental samples.[139] Besides, Dan Liao *et al.* used *in situ* nucleation and conversion of ZIF-8 on 2D hierarchical Ti_3C_2 MXene nanosheets to effectively synthesize a novel composite, N-Ti_3C_2/PC. The addition of ZIF-8 greatly enhanced the electrochemical properties of the composite and stopped the restacking of the Ti_3C_2 nanosheets. An electrochemical sensor was constructed for the detection of 4-aminophenol (4-AP) using the N-Ti_3C_2/PC composite. Because N-Ti_3C_2 and PC worked in concert to speed up electron transfer on the electrode surface, this sensor showed outstanding electrocatalytic activity for 4-AP. The developed electrochemical sensor displayed an excellent linear response of 1–150 μM with a low limit of detection of 0.059 μM for 4-AP in the presence of different foreign interferent species. Thus, it is anticipated that the N-Ti_3C_2/PC composite will find diverse applications in electrochemical sensing for the detection of environmental pollutants in wastewater systems.[140] Furthermore, Sanko and coworkers created an electrochemical sensor using an $Mo_2Ti_2AlC_3$/MWCNT (multi-walled carbon nanotube) nanocomposite. $Mo_2Ti_2AlC_3$ was used to create the MAX phase of the sensor, and MWCNT was used to increase the conductivity and sensitivity. Utilizing differential pulse voltammetry and cyclic voltammetry, the electrochemical capabilities of the sensor were assessed (DPV). The outcomes demonstrated that the $Mo_2Ti_2AlC_3$/MWCNT nanocomposite demonstrated a single, diffusion-controlled, irreversible oxidation process against BPA. The sensor also had a linear working range of 0.01–8.50 M determined from DPV, and an LOD of 2.7 nM and 8.91 nM, as shown in Fig. 12(a and b). However, the composite exhibited a single oxidation process in response to BPA, characterized by diffusion control and irreversibility. Also, the sensor was effectively employed for the quantification of BPA in milk packaging, plastic bottles, and cans, demonstrating recoveries in the range of 95.67% to 100.60%. Furthermore, the performance of this sensor was assessed through studies on selectivity, repeatability, and reusability, as shown in Fig. 12(c and d). This study not only introduces a novel approach to propel research on MAX phase materials for electrochemical detection across various

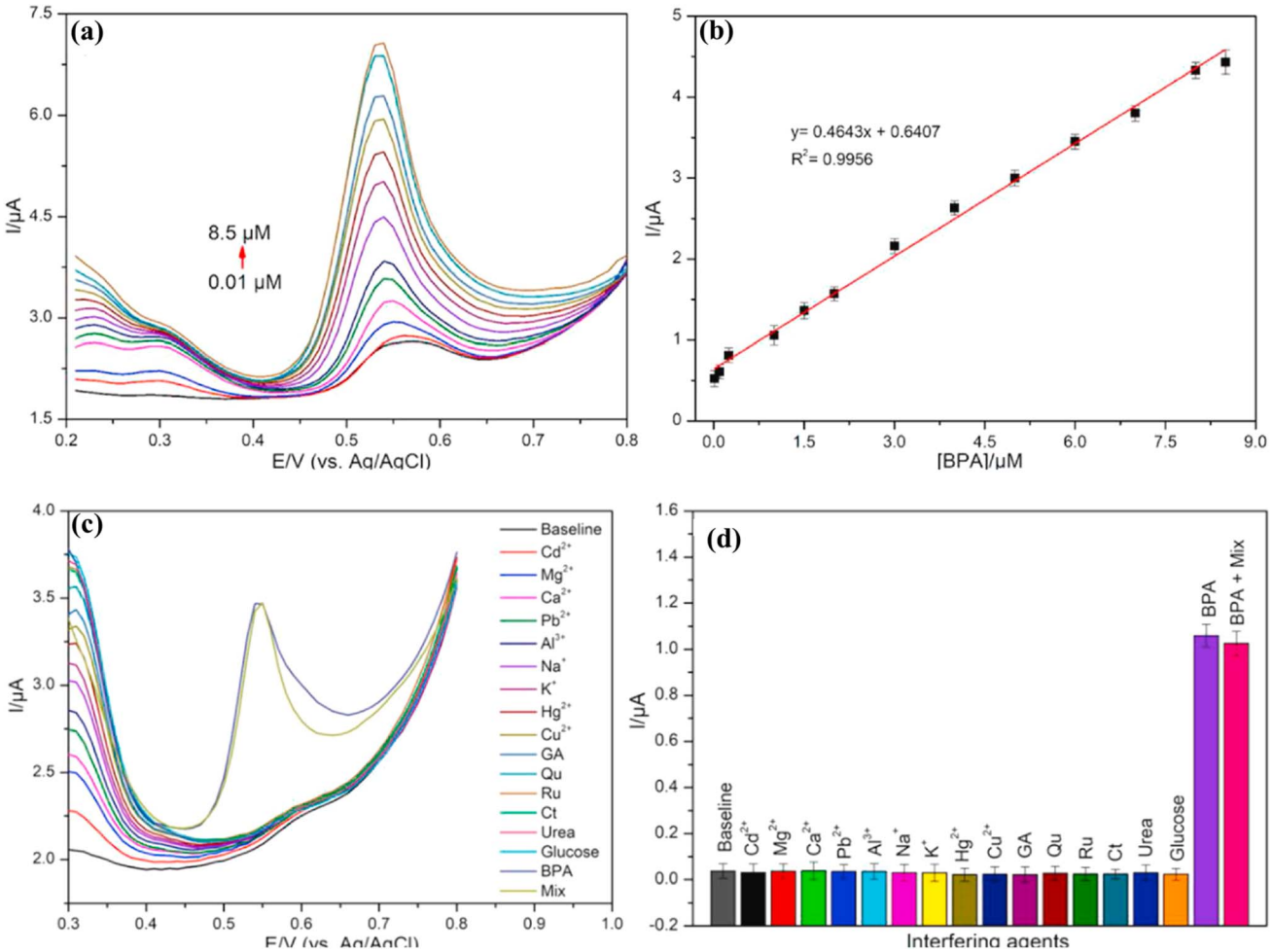

Fig. 12 (a) DPV responses at different concentrations of BPA on $Mo_2Ti_2AlC_3$/MWCNT/GCE and (b) the linear relationship between current and concentration of BPA. (c and d) Selective determination of BPA. Reproduced from ref. 141. Copyright (2022), adopted with permission from Elsevier.

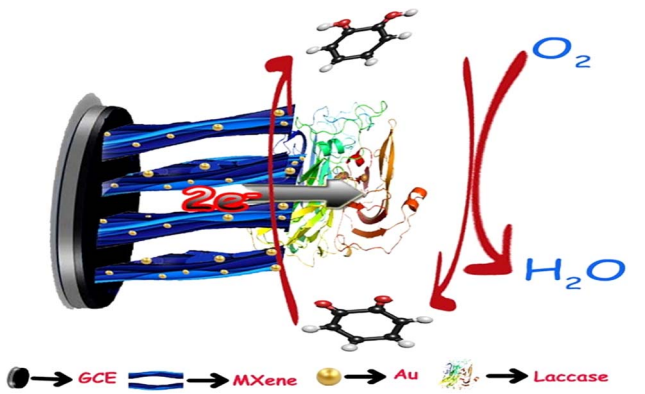

Fig. 13 Schematic of Lac/Au/MXene/GCE-catalyzed oxidation of catechol.[143] Copyright (2021), adopted from Elsevier.

analytes but also presents a highly effective electrochemical alternative for the detection of BPA in real samples.[141]

Rajendran *et al.* aimed to create an electrochemical sensor for the detection of bisphenol A (BPA) using a top-down approach. They developed a 2D mixed graphene/$Ti_3C_2T_x$ nanocomposite (Gr/MXene) for this purpose. The successful formation of graphene sheets with MXene was verified through X-ray diffraction spectroscopy (XRD) and Raman spectroscopy analysis. High-resolution scanning electron microscopy (HR-SEM) was employed to confirm the formation of both MXene and the Gr/MXene nanocomposite. The researchers utilized a Gr/MXene nanocomposite-modified glassy carbon electrode (GCE) for the oxidation of BPA in a 100 mM phosphate buffer solution (PBS) to develop an electrochemical sensor to monitor BPA. Gr/MXene/GCE demonstrated linear detection limits of 4.08 nM and 0.35 mM for BPA, as determined by differential pulse voltammetry (DPV). The linear detection range was 10 to 180 nM and 1 to 10 mM for BPA. Additionally, this sensor demonstrated good repeatability, selectivity, stability, and consistency for the detection of BPA. The researchers successfully utilized the Gr/MXene-modified sensor to detect BPA in contemporary plastic products, achieving a recovery rate in the range of 99.2% to 104.5%. Overall, this study introduces an electrochemical sensor with sensitivity and specificity for the detection of BPA, which can have a significant impact on food

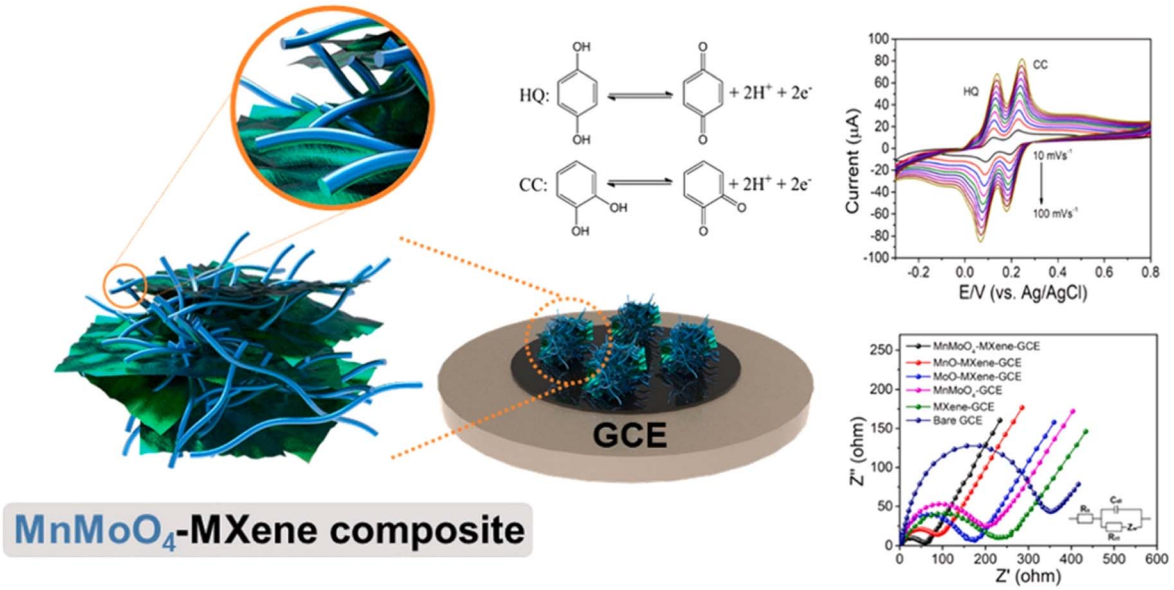

Fig. 14 Modification of the surface of GCE using the $MnMoO_4$-MXene nanocomposite material for the detection of hydroquinone and catechol.[145] Copyright, adopted from Elsevier.

and environmental safety.[142] In the study by Chandran *et al.*, a glassy carbon electrode (GCE) was immobilized with laccase (Lac) on Au/MXene to create a sensing electrode, as shown in Fig. 13. X-ray diffraction (XRD), scanning electron microscopy (SEM), and energy-dispersive X-ray spectroscopy were used to characterize the synthesized Au/MXene substance. Moreover, the adsorbed enzymes could still function as biological electrocatalysts because the Au nanoparticles enabled the transfer of electrons between the Au surface and the T1 copper site of the electroactive laccase. With a comparatively high sensitivity of 0.05 mA mM^{-1} and a detection limit of 0.05 mM, the Lac/Au/MXene/GCE electrode was used to study the electrochemical oxidation of catechol. This electrode showed a perfectly linear amperometric response in the concentration range of 0.05 to 0.15 mM. Moreover, the sensor electrode demonstrated outstanding repeatability, reproducibility, and durability. Therefore, the Lac/Au/MXene/GCE developed sensor system was proven to be highly effective in detecting catechol in industrial effluents and water bodies, offering a valuable means to mitigate environmental pollution.[143]

Huang and colleagues modified functional groups on the surface of Ti_3C_2 by alkalization treatment to create new electrode materials. Unfortunately, practical applications face major difficulties when trying to stack Ti_3C_2 sheets. An innovative self-assembling technique was created to build a heterostructure made of MOF and Ti_3C_2 to overcome this restriction. Alk- Ti_3C_2 was combined with nitrogen-doped porous carbon (N-PC) produced from MOF-5-NH_2 to create the structure, which is known as alk-Ti_3C_2/N-PC. The latter was created by treating Ti_3C_2 by acid etching and alkaline intercalation. This method successfully stopped the Ti_3C_2 sheets from stacking again, enabling the detection of benzenediol *via* hydrogen-bond contact. The abundance of OH functional groups on alk-Ti_3C_2 and the large number of CeN bonds on N-PC caused this interaction. Using the benzenediol/benzoquinone redox reactions to detect hydroquinone (HQ) and catechol (CT), the alk-Ti_3C_2/N-PC electrode had good conductivity and surface area. With a low detection limit of 4.8 nM (S/N = 3) for HQ and CT, respectively, and a broad linear detection range of 0.5–150 M under ideal conditions, this electrode demonstrated an excellent performance. It also showed outstanding reproducibility and durability. Moreover, the alk-Ti_3C_2/N-PC electrochemical sensor was used to detect HQ and CT in industrial wastewater, with acceptable recoveries, to evaluate the viability of the electrode for environmental analysis. In conclusion, decorating alk-Ti_3C_2 with N-PC is a novel technique for developing different alk-Ti_3C_2-based composites that can identify phenolic isomers and examine environmental materials.[144] Moreover, Ranjith *et al.* created a composite electrochemical sensor with a few-layered exfoliated two-dimensional (2D) MXene and one-dimensional (1D) $MnMoO_4$ nanofibers. The 1D $MnMoO_4$ and 2D MXene nanoarchitecture were created to improve the electrocatalytic activity and synergistic signal enhancement for the oxidation of HQ and CC, as shown in Fig. 14. The synthesized $MnMoO_4$-MXene-GCE sensor displayed oxidation potentials of 0.102 V and 0.203 V for HQ and CC, respectively. It also had a distinct and simultaneous sensing range of 0.101 V and a powerful anodic peak current. With low detection limits of 0.26 nM and 0.30 nM, respectively, the developed 1D–2D hybridised $MnMoO_4$-MXene-GCE sensor showed a broad linear response of 5 nM to 65 nM for both HQ and CC. Additionally, the sensor showed significant stability. The 1D–2D $MnMoO_4$-MXene nanocomposite-based biosensor successfully detected HQ and CC in hazardous water pollutants, and the recovery values were obtained using the differential pulse voltammetric method. Therefore, it was deduced that $MnMoO_4$-MXene-GCE is

suitable for sensing HQ and CC in wastewater samples, showing promise as a sensing platform for HQ and CC in wastewater samples.[145]

Tingting Yu and colleagues focused on creating electrode materials that can perform double roles as pollutant monitors in wastewater systems. A two-step method was used in this study to successfully synthesize the novel electrode material V_2CT_x@NiCoMn-OH. Using ZIF-67 as a framework and basic anion exchange, a three-dimensional (3D) hollow structure of NiCoMn–OH was first created. Also, the NiCoMn–OH structure was combined with the 2D layered V_2CT_x MXene in the subsequent phase. The self-accumulation of the MXene nanosheets was successfully constrained by intercalating the NiCoMn–OH structure with the V_2CT_x MXene, and a 3D cross-linked hollow structure was created. This structure increased the conductivity of NiCoMn-OH, revealed more active sites of V_2CT_x@NiCoMn-OH, and widened the ion transport channel. Moreover, the developed electrochemical sensor showed a good linear response of 2–1050 μM with a low limit of detection of 0.559 μM for hydroquinone in wastewater. Moreover, the V_2CT_x@-NiCoMn-OH-20 electrode demonstrated noteworthy electrocatalytic efficacy towards hydroquinone, encompassing elevated sensitivity, excellent selectivity, a low detection limit, and a broad linear range. Consequently, these exceptional performance metrics indicate that the devised approach for the successful fabrication of V_2CT_x@NiCoMn-OH-20 can potentially establish a novel avenue for the advancement of dual-functional electrode materials tailored for the environmental monitoring of different pollutants in the aquatic environment.[146]

5. Conclusion and future perspective

In conclusion, the diverse synthesis methods employed in the development of MXene-based nanocomposites have significantly expanded the landscape of materials available for the fabrication of electrochemical sensors. The versatility in synthesis techniques, including chemical etching, intercalation, and exfoliation, allows the tailoring of the structural and compositional characteristics of MXene nanocomposites, enhancing their performance as electrochemical sensors. The ability to fine-tune these materials has opened up new avenues for detecting environmental pollutants such as heavy metals, organic pesticides, and antibiotic drugs with unprecedented sensitivity and selectivity. Although the current research landscape predominantly focuses on the electrochemical sensing applications of MXene-based nanocomposites, there is a need for a paradigm shift towards addressing the challenges associated with scalability, cost-effectiveness, and real-world applicability. Future research endeavors should strive to optimize synthesis methods for large-scale production, while maintaining the desirable properties that make MXene nanocomposites suitable for electrochemical sensing. This shift is crucial for the practical implementation of these sensors in monitoring environmental pollutants on a broader scale. Furthermore, the integration of artificial intelligence (AI) in the field holds immense potential. AI algorithms can enhance the efficiency and accuracy of pollutant detection by analyzing complex datasets generated from electrochemical sensors. Machine learning models can adapt and learn from diverse environmental conditions, leading to more robust and reliable sensor systems. Collaborative efforts between material scientists, electrochemists, and data scientists will play a pivotal role in developing intelligent sensor platforms capable of real-time monitoring and early detection of environmental pollutants.

In the future, MXene-based nanocomposites have the potential to revolutionize environmental monitoring by providing cost-effective, scalable, and AI-enhanced solutions for pollutant detection. As technology advances, these sensors may find widespread use in industrial settings, water treatment facilities, and even wearable devices for personal environmental monitoring. The synthesis methods and applications explored thus far lay the foundation for a promising future where MXene-based nanocomposites contribute significantly to mitigating the impact of environmental pollutants on the ecosystem and human health. The convergence of materials science, electrochemistry, and artificial intelligence holds the key to unlocking the full potential of MXene-based nanocomposites in environmental sensing.

Data availability

The authors confirm that the data supporting the findings of this study are available within the article.

Conflicts of interest

The authors declare that they have no competing interests or personal relationships with anyone that could have influenced the work reported in this review paper.

Acknowledgements

The authors are thankful to Prof. Yury Gogotsi, A. J. Drexel Nanomaterials Institute, Department of Materials Science and Engineering, Drexel, USA. Ali Hyder acknowledges the financial support from the Higher Education of Pakistan, Islamabad, Pakistan, through the Indigenous Fellowship 5000, Phase II, Batch VI.

References

1 N. Gaur, S. Sharma and N. Yadav, in *Green Chemistry Approaches to Environmental Sustainability*, Elsevier, 2024, pp. 23–41.
2 A. Hyder, A. Ali, A. Khalid, A. Nadeem, M. A. Khan, A. W. Memon, A. A. Memon, D. Janwery, M. Mehdi, A. Solangi, J. Yang and K. H. Thebo, *Ind. Eng. Chem. Res.*, 2023, **62**, 21335–21346.
3 F. Rehman, F. Hussain Memon, S. Ullah, M. A. Jafar Mazumder, A. Al-Ahmed, F. Khan and K. Hussain Thebo, *Chem. Rec.*, 2022, **22**, e202200107.
4 S. Wang, Y. Li, Q. Liu, J. Wang, Y. Zhao, Y. Cai, H. Li and Z. Chen, *J. Photochem. Photobiol., A*, 2023, **437**, 114435.

5 M.-U.-N. Khilji, A. A. Otho, R. Memon, A. Khalid, M. Kazi, A. Hyder, D. Janwery, N. A. Nahyoon, A. A. Memon and N. Memon, *Anal. Lett.*, 2023, 1–18.
6 J. A. Buledi, A. H. Pato, A. H. Kanhar, A. R. Solangi, M. Batool, S. Ameen and I. M. Palabiyik, *Appl. Nanosci.*, 2021, **11**, 1241–1256.
7 T. A. Bhutto, M. A. Jakhrani, A. A. Jamali, J. A. Buledi, R. D. Janwary, A. Hyder, K. H. Chachar and N. H. Kalwar, *J. Iran. Chem. Soc.*, 2023, 1–11.
8 A. Hyder, J. A. Buledi, M. Nawaz, D. B. Rajpar, Y. Orooji, M. L. Yola, H. Karimi-Maleh, H. Lin and A. R. Solangi, *Environ. Res.*, 2022, **205**, 112475.
9 W.-L. Jia, C. Song, L.-Y. He, B. Wang, F.-Z. Gao, M. Zhang and G.-G. Ying, *Curr. Opin. Environ. Sci. Health*, 2023, **32**, 100437.
10 W. Wang, P. Xiong, H. Zhang, Q. Zhu, C. Liao and G. Jiang, *Environ. Res.*, 2021, **201**, 111531.
11 S. Ali, M. I. Ullah, A. Sajjad, Q. Shakeel and A. Hussain, *Sustain. Agric. Rev.*, 2021, **2**, 311–336.
12 F. A. Janjhi, I. Chandio, D. Janwery, A. A. Memon, K. H. Thebo, G. Boczkaj, V. Vatanpour and R. Castro-Muñoz, *Chem. Eng. Res. Des.*, 2023, **199**, 327–347.
13 A. Qadeer, Z. A. Saqib, Z. Ajmal, C. Xing, S. K. Khalil, M. Usman, Y. Huang, S. Bashir, Z. Ahmad and S. Ahmed, *Sustain. Cities Soc.*, 2020, **53**, 101959.
14 G. L. Silveira, M. G. F. Lima, G. B. Dos Reis, M. J. Palmieri and L. F. Andrade-Vieria, *Chemosphere*, 2017, **178**, 359–367.
15 S. Wasi, S. Tabrez and M. Ahmad, *Environ. Monit. Assess.*, 2013, **185**, 2585–2593.
16 Z. Fu and S. Xi, *Toxicol. Mech. Methods*, 2020, **30**, 167–176.
17 F. A. Janjhi, D. Janwery, I. Chandio, S. Ullah, F. Rehman, A. A. Memon, J. Hakami, F. Khan, G. Boczkaj and K. H. Thebo, *ChemBioEng Rev.*, 2022, **9**, 574–590.
18 D. Janwery, F. H. Memon, A. A. Memon, M. Iqbal, F. N. Memon, W. Ali, K. H. Choi and K. H. Thebo, *ACS omega*, 2022, **8**(8), 7648–7656.
19 D. Witkowska, J. Słowik and K. Chilicka, *Molecules*, 2021, **26**, 6060.
20 K. G. Pavithra, P. Sundarrajan, J. Arun, K. Brindhadevi, Q. H. Le and A. Pugazhendhi, *Environ. Res.*, 2023, 117005.
21 A. Labidi, H. Ren, A. Sial, H. Wang, E. Lichtfouse and C. Wang, *Crit. Rev. Environ. Sci. Technol.*, 2023, 1–24.
22 I. El-Nahhal and Y. El-Nahhal, *J. Environ. Manage.*, 2021, **299**, 113611.
23 A. Saravanan, P. S. Kumar, S. Jeevanantham, M. Anubha and S. Jayashree, *Environ. Pollut.*, 2022, **298**, 118844.
24 A. Hyder, M. Thebo, D. Janwery, J. A. Buledi, I. Chandio, A. Khalid, B. S. Al-Anzi, H. A. Almukhlifi, K. H. Thebo and F. N. Memon, *Heliyon*, 2023, **9**, e19622.
25 A. A. Chandio, S. Memon, A. A. Memon, A. Balouch, R. Memon, K. H. Thebo, F. N. Memon, M. H. Agheem, S. S. Memon and A. A. Otho, *Polycyclic Aromat. Compd.*, 2023, **43**, 4843–4855.
26 S. Panhwar, J. A. Buledi, D. Mal, A. R. Solangi, A. Balouch and A. Hyder, *Curr. Anal. Chem.*, 2021, **17**, 1169–1181.
27 T. Ahmad, M. Rafatullah, A. Ghazali, O. Sulaiman, R. Hashim and A. Ahmad, *J. Environ. Sci. Health, Part C:Environ. Carcinog. Ecotoxicol. Rev.*, 2010, **28**, 231–271.
28 C. Li and L. Chen, *Chromatographia*, 2013, **76**, 409–417.
29 E. Bozorgzadeh, A. Pasdaran and H. Ebrahimi-Najafabadi, *Food Chem.*, 2021, **346**, 128916.
30 S. Sagbas, C. Kantar and N. Sahiner, *Water, Air, Soil Pollut.*, 2014, **225**, 1–10.
31 M. A. Abedalwafa, Y. Li, C. Ni and L. Wang, *Anal. Methods*, 2019, **11**, 2836–2854.
32 M. Marimuthu, S. S. Arumugam, D. Sabarinathan, H. Li and Q. Chen, *Trends Food Sci. Technol.*, 2021, **116**, 1002–1028.
33 A. Hyder, S. S. Memon, J. A. Buledi, S. Memon, Z.-u.-A. Memon, D. B. Rajpar and Sirajuddin, *Anal. Sci.*, 2023, **39**, 1981–1992.
34 J. J. A. Buledi, A. R. Solangi, A. Hyder, M. Batool, N. Mahar, A. Mallah, H. Karimi-Maleh, O. Karaman, C. Karaman and M. Ghalkhani, *Environ. Res.*, 2022, **212**, 113372.
35 A. Hyder, S. S. Memon, S. Memon, D. B. Rajpar, S. G. Shaikh and J. A. Buledi, *Microchem. J.*, 2021, **163**, 105908.
36 A. Hyder, S. S. Memon, J. A. Buledi, S. Memon, Z.-u.-A. Memon, S. G. Shaikh and D. B. Rajpar, *Chem. Pap.*, 2023, **77**, 7737–7748.
37 A. Hyder, J. A. Buledi, R. Memon, A. Qureshi, J. H. Niazi, A. R. Solangi, S. Memon, A. A. Memon and K. H. Thebo, *Diamond Relat. Mater.*, 2023, **139**, 110357.
38 M. Nawaz, H. Shaikh, J. A. Buledi, A. R. Solangi, C. Karaman, N. Erk, R. Darabi and M. B. Camarada, *Carbon Lett.*, 2023, 1–14.
39 J. A. Buledi, A. Hyder, A. R. Solangi, R. Darabi and H. Karimi-Maleh, *Inorg. Chem. Commun.*, 2023, 111934.
40 J. A. Buledi, A. R. Solangi, A. Mallah, S. Amin and E. A. López-Maldonado, *Diamond Relat. Mater.*, 2024, 110801.
41 J. A. Buledi and A. R. Solangi, *Chem. Pap.*, 2023, **77**, 6377–6386.
42 M. Nawaz, H. Shaikh, J. A. Buledi, A. R. Solangi, R. Raza and B. Maher, *J. Appl. Electrochem.*, 2023, **53**, 751–764.
43 L. Liu, Y. Zhou, S. Liu and M. Xu, *ChemElectroChem*, 2018, **5**, 6–19.
44 C. B. Jacobs, M. J. Peairs and B. J. Venton, *Anal. Chim. Acta*, 2010, **662**, 105–127.
45 X. Zhan, C. Si, J. Zhou and Z. Sun, *Nanoscale Horiz.*, 2020, **5**, 235–258.
46 I. Mahar, F. H. Memon, J.-W. Lee, K. H. Kim, R. Ahmed, F. Soomro, F. Rehman, A. A. Memon, K. H. Thebo and K. H. Choi, *Membranes*, 2021, **11**, 869.
47 J. Yang, W. Bao, P. Jaumaux, S. Zhang, C. Wang and G. Wang, *Adv. Mater. Interfaces*, 2019, **6**, 1802004.
48 H. Ali, A. Ali, J. A. Buledi, A. A. Memon, A. R. Solangi, J. Yang and K. H. Thebo, *Mater. Chem. Front.*, 2023, **7**, 5519–5544.
49 S. Sharif, K. S. Ahmad, F. Rehman, Z. Bhatti and K. H. Thebo, *J. Environ. Chem. Eng.*, 2021, **9**, 105605.
50 A. Ali, M. Aamir, K. H. Thebo and J. Akhtar, *Chem. Rec.*, 2020, **20**, 344–354.
51 Z. Huang, X. Yuan and X. Liu, *J. Hydrol.*, 2021, **601**, 126658.

52 I. Mahar, F. K. Mahar, N. Mahar, A. A. Memon, A. A. A. Pirzado, Z. Khatri, K. H. Thebo and A. Ali, *Chem. Eng. Res. Des.*, 2023, **191**, 462–471.
53 R. Bhardwaj and A. Hazra, *J. Mater. Chem. C*, 2021, **9**, 15735–15754.
54 Z. Ahmed, F. Rehman, U. Ali, A. Ali, M. Iqbal and K. H. Thebo, *ChemBioEng Rev.*, 2021, **8**, 110–120.
55 U. Noor, M. F. Mughal, T. Ahmed, M. F. Farid, M. Ammar, U. Kulsum, A. Saleem, M. Naeem, A. Khan and A. Sharif, *Nanotechnology*, 2023, **34**, 262001.
56 Z. Zou, Q. Wang, J. Yan, K. Zhu, K. Ye, G. Wang and D. Cao, *ACS Nano*, 2021, **15**, 12140–12150.
57 P. Kuang, J. Low, B. Cheng, J. Yu and J. Fan, *J. Mater. Sci. Technol.*, 2020, **56**, 18–44.
58 N. H. Solangi, N. M. Mubarak, R. R. Karri, S. A. Mazari, S. K. Kailasa and A. Alfantazi, *Chemosphere*, 2023, **314**, 137643.
59 T. S. Gopal, S. K. Jeong, T. A. Alrebdi, S. Pandiaraj, A. Alodhayb, M. Muthuramamoorthy and A. N. Grace, *Mater. Today Chem.*, 2022, **24**, 100891.
60 K. Velusamy, P. Chellam, P. S. Kumar, J. Venkatachalam, S. Periyasamy and R. Saravanan, *Environ. Pollut.*, 2022, **301**, 119034.
61 M. Mozafari and M. Soroush, *Mater. Adv.*, 2021, **2**, 7277–7307.
62 S. Jung, U. Zafar, L. S. K. Achary and C. M. Koo, *EcoMat*, 2023, **5**, e12395.
63 G. Yang, X. Hu, J. Liang, Q. Huang, J. Dou, J. Tian, F. Deng, M. Liu, X. Zhang and Y. Wei, *J. Hazard. Mater.*, 2021, **419**, 126220.
64 R. Fang, C. Lu, A. Chen, K. Wang, H. Huang, Y. Gan, C. Liang, J. Zhang, X. Tao and Y. Xia, *ChemSusChem*, 2020, **13**, 1409–1419.
65 I. Amin, H. v. d. Brekel, K. Nemani, E. Batyrev, A. de Vooys, H. van der Weijde, B. Anasori and N. R. Shiju, *ACS Appl. Mater. Interfaces*, 2022, **14**, 43749–43758.
66 M. Naguib, V. N. Mochalin, M. W. Barsoum and Y. Gogotsi, *Adv. Mater.*, 2014, **26**, 992–1005.
67 M. W. Barsoum, *Prog. Solid State Chem.*, 2000, **28**, 201–281.
68 M. Naguib, M. Kurtoglu, V. Presser, J. Lu, J. Niu, M. Heon, L. Hultman, Y. Gogotsi and M. W. Barsoum, *Adv. Mater.*, 2011, **23**, 4248–4253.
69 X. Sang, Y. Xie, M.-W. Lin, M. Alhabeb, K. L. Van Aken, Y. Gogotsi, P. R. Kent, K. Xiao and R. R. Unocic, *ACS Nano*, 2016, **10**, 9193–9200.
70 P. Urbankowski, B. Anasori, T. Makaryan, D. Er, S. Kota, P. L. Walsh, M. Zhao, V. B. Shenoy, M. W. Barsoum and Y. Gogotsi, *Nanoscale*, 2016, **8**, 11385–11391.
71 B. C. Wyatt, A. Rosenkranz and B. Anasori, *Adv. Mater.*, 2021, **33**, 2007973.
72 M. Alhabeb, K. Maleski, B. Anasori, P. Lelyukh, L. Clark, S. Sin and Y. Gogotsi, *Chem. Mater.*, 2017, **29**, 7633–7644.
73 M. Ghidiu, M. R. Lukatskaya, M.-Q. Zhao, Y. Gogotsi and M. W. Barsoum, *Nature*, 2014, **516**, 78–81.
74 X. Wang, C. Garnero, G. Rochard, D. Magne, S. Morisset, S. Hurand, P. Chartier, J. Rousseau, T. Cabioc'h and C. Coutanceau, *J. Mater. Chem. A*, 2017, **5**, 22012–22023.
75 S.-Y. Pang, Y.-T. Wong, S. Yuan, Y. Liu, M.-K. Tsang, Z. Yang, H. Huang, W.-T. Wong and J. Hao, *J. Am. Chem. Soc.*, 2019, **141**, 9610–9616.
76 P. Urbankowski, B. Anasori, K. Hantanasirisakul, L. Yang, L. Zhang, B. Haines, S. J. May, S. J. Billinge and Y. Gogotsi, *Nanoscale*, 2017, **9**, 17722–17730.
77 P. Paul, P. Chakraborty, T. Das, D. Nafday and T. Saha-Dasgupta, *Phys. Rev. B*, 2017, **96**, 035435.
78 M. Khazaei, M. Arai, T. Sasaki, C. Y. Chung, N. S. Venkataramanan, M. Estili, Y. Sakka and Y. Kawazoe, *Adv. Funct. Mater.*, 2013, **23**, 2185–2192.
79 M. Naguib, O. Mashtalir, J. Carle, V. Presser, J. Lu, L. Hultman, Y. Gogotsi and M. W. Barsoum, *ACS Nano*, 2012, **6**, 1322–1331.
80 M. Alhabeb, K. Maleski, T. S. Mathis, A. Sarycheva, C. B. Hatter, S. Uzun, A. Levitt and Y. Gogotsi, *Angew. Chem.*, 2018, **130**, 5542–5546.
81 H. L. Chia, C. C. Mayorga-Martinez, N. Antonatos, Z. k. Sofer, J. J. Gonzalez-Julian, R. D. Webster and M. Pumera, *Anal. Chem.*, 2020, **92**, 2452–2459.
82 H. Wang, J. Zhang, Y. Wu, H. Huang, G. Li, X. Zhang and Z. Wang, *Appl. Surf. Sci.*, 2016, **384**, 287–293.
83 A. Sinha, B. Tan, Y. Huang, H. Zhao, X. Dang, J. Chen and R. Jain, *TrAC, Trends Anal. Chem.*, 2018, **102**, 75–90.
84 E. Satheeshkumar, T. Makaryan, A. Melikyan, H. Minassian, Y. Gogotsi and M. Yoshimura, *Sci. Rep.*, 2016, **6**, 32049.
85 L. Lorencova, T. Bertok, J. Filip, M. Jerigova, D. Velic, P. Kasak, K. A. Mahmoud and J. Tkac, *Sens. Actuators, B*, 2018, **263**, 360–368.
86 R. Rakhi, P. Nayak, C. Xia and H. N. Alshareef, *Sci. Rep.*, 2016, **6**, 36422.
87 J. Dong, X. Li, L. Wen, Y. Ma, J. Xu, H. Luo, J. Hou, C. Hou and D. Huo, *Food Chem.*, 2024, **437**, 137835.
88 H. Yao, R. Wu, J. Zou, J. Liu, G. Peng, X. Wang, W. Zhou, S. Ai and L. Lu, *Chemosphere*, 2023, **340**, 139728.
89 H. Yao, R. Wu, J. Zou, J. Liu, G. Peng, X. Wang, W. Zhou, S. Ai and L. Lu, *Chemosphere*, 2023, **340**, 139728.
90 M. Akhtar, M. Sohail, M. F. Warsi, M. M. Ibrahim, M. A. Amin and M. Shahid, *FlatChem*, 2023, **41**, 100537.
91 H. Cheng and J. Yang, *Int. J. Electrochem. Sci.*, 2020, **15**, 2295–2306.
92 P. Xiao, G. Zhu, X. Shang, B. Hu, B. Zhang, Z. Tang, J. Yang and J. Liu, *J. Electroanal. Chem.*, 2022, **916**, 116382.
93 S. Bagheri, R. Chilcott, S. Luo and A. Sinitskii, *Langmuir*, 2022, **38**, 12924–12934.
94 X. Guo, Y. Zhang, H. Ge, J. Zhang, P. Yang and Z. Wu, *J. Electroanal. Chem.*, 2023, **935**, 117320.
95 P. A. Rasheed, R. P. Pandey, T. Gomez, M. Naguib and K. A. Mahmoud, *RSC Adv.*, 2020, **10**, 24697–24704.
96 Y. He, L. Ma, L. Zhou, G. Liu, Y. Jiang and J. Gao, *Nanomaterials*, 2020, **10**, 866.
97 X. Zhu, B. Liu, H. Hou, Z. Huang, K. M. Zeinu, L. Huang, X. Yuan, D. Guo, J. Hu and J. Yang, *Electrochim. Acta*, 2017, **248**, 46–57.
98 Y. Chen, P. Zhao, Y. Liang, Y. Ma, Y. Liu, J. Zhao, J. Hou, C. Hou and D. Huo, *Talanta*, 2023, **256**, 124294.

99 L. Wen, J. Dong, H. Yang, J. Zhao, Z. Hu, H. Han, C. Hou, X. Luo and D. Huo, *Sci. Total Environ.*, 2022, **851**, 158325.
100 X. Zhang, D. An, Z. Bi, W. Shan, B. Zhu, L. Zhou, L. Yu, H. Zhang, S. Xia and M. Qiu, *J. Electroanal. Chem.*, 2022, **911**, 116239.
101 X. Zhu, B. Liu, L. Li, L. Wu, S. Chen, L. Huang, J. Yang, S. Liang, K. Xiao and J. Hu, *Microchim. Acta*, 2019, **186**, 1–7.
102 J. A. Buledi, A. R. Solangi, A. Mallah, Z.-u.-H. Shah, S. T. Sherazi, M. R. Shah, A. Hyder and S. Ali, *J. Food Meas. Charact.*, 2023, **17**, 1628–1639.
103 I. Mahmood, S. R. Imadi, K. Shazadi, A. Gul and K. R. Hakeem, *Plant, soil and microbes: volume 1: implications in crop science*, 2016, pp. 253–269.
104 K.-H. Kim, E. Kabir and S. A. Jahan, *Sci. Total Environ.*, 2017, **575**, 525–535.
105 J. A. Buledi, M. Batool, S. Ameen, A. R. Solangi, A. Mallah, I. M. Palaybik, S. T. H. Sherazi and S. Ali, *Chem. Pap.*, 2023, **77**, 7215–7223.
106 Y. Jiang, X. Zhang, L. Pei, S. Yue, L. Ma, L. Zhou, Z. Huang, Y. He and J. Gao, *Chem. Eng. J.*, 2018, **339**, 547–556.
107 W. Zhong, J. Zou, Q. Yu, Y. Gao, F. Qu, S. Liu, H. Zhou and L. Lu, *Food Chem.*, 2023, **402**, 134379.
108 X. Tu, F. Gao, X. Ma, J. Zou, Y. Yu, M. Li, F. Qu, X. Huang and L. Lu, *J. Hazard. Mater.*, 2020, **396**, 122776.
109 W. Zhong, F. Gao, J. Zou, S. Liu, M. Li, Y. Gao, Y. Yu, X. Wang and L. Lu, *Food Chem.*, 2021, **360**, 130006.
110 Y. Mi, Y. Zhao, J. Chen, X. Li, Y. Yang and F. Gao, *J. Hazard. Mater.*, 2022, **438**, 129419.
111 W. Zhong, J. Zou, Y. Xie, J. Yang, M. Li, S. Liu, Y. Gao, X. Wang and L. Lu, *J. Electroanal. Chem.*, 2022, **920**, 116586.
112 F. Zhao, Y. Yao, C. Jiang, Y. Shao, D. Barceló, Y. Ying and J. Ping, *J. Hazard. Mater.*, 2020, **384**, 121358.
113 Y. He, X. Zhou, L. Zhou, X. Zhang, L. Ma, Y. Jiang and J. Gao, *Ind. Eng. Chem. Res.*, 2020, **59**, 15556–15564.
114 A. Sinha, K. Ma and H. Zhao, *J. Colloid Interface Sci.*, 2021, **590**, 365–374.
115 D. Song, X. Jiang, Y. Li, X. Lu, S. Luan, Y. Wang, Y. Li and F. Gao, *J. Hazard. Mater.*, 2019, **373**, 367–376.
116 W. Guo, L. Liang, Y. Zhao, C. Zhao, X. Lu, Y. Cao and F. Gao, *Colloids Surf., B*, 2023, **224**, 113238.
117 R. Ding, W. Jiang, Y. Ma, Q. Yang, X. Han and X. Hou, *Microchem. J.*, 2023, **187**, 108425.
118 J. Yang, C. Deng, W. Zhong, G. Peng, J. Zou, Y. Lu, Y. Gao, M. Li, S. Zhang and L. Lu, *Microchim. Acta*, 2023, **190**, 146.
119 S. Chen, J. Zou, X. Pan, S. Zeng, Y. Liu, J. Ye, L. Lu, S. Yang and G. Zhan, *Molecules*, 2023, **28**, 7347.
120 E. Hou, Z. Kong, J. Wu, H. Wang, P. Nie, M. Lu and L. Chang, *J. Mater. Sci.: Mater. Electron.*, 2023, **34**, 1177.
121 F. Yu, Y. Li, S. Han and J. Ma, *Chemosphere*, 2016, **153**, 365–385.
122 D. Balarak, A. D. Khatibi and K. Chandrika, *Int. J. Pharm. Invest.*, 2020, **10**, 106–111.
123 A. Chen, Y. Wei, D. Tuo, C. Zhou, S. Shi, N. Tang, Q. He and J. Liu, *J. Alloys Compd.*, 2024, **970**, 172557.
124 Z. Yang, J. Hu, X. Zhang, H. Yang, P. Meng, H. Zhao and Y. Sun, *Anal. Bioanal. Chem.*, 2023, **415**, 157–166.
125 R. K. Devi, M. Ganesan, T.-W. Chen, S.-M. Chen, A. M. Abbasi, M. A. Ali, M. S. Elshikh, J. Yu, H.-Y. Chuang and B. Xu, *Chem. Eng. J.*, 2023, **474**, 145693.
126 R. Rajakumaran, J. Anupriya and S.-M. Chen, *Mater. Lett.*, 2021, **297**, 129979.
127 M. I. Shekh, K. Shahzadi, Y. Liu, X. Yan, Q. Li, W. Xiong, D. M. Patel, F. J. Stadler and G. Zhu, *Microchem. J.*, 2024, **197**, 109658.
128 S. H. Tumrani, R. R. Neiber, Z. Pitafi, I. A. Ahmed, R. A. Soomro, M. M. Ibrahim, S. Karakuş and Z. M. El-Bahy, *J. Environ. Chem. Eng.*, 2023, **11**, 111152.
129 A. E. Vilian, S.-K. Hwang, G. Bhaskaran, M. Alhammadi, S. Kim, J. N. Tiwari, Y. S. Huh and Y.-K. Han, *Chem. Eng. J.*, 2023, **454**, 139980.
130 R. K. Devi, M. Ganesan, T.-W. Chen, S.-M. Chen, M. Akilarasan, S.-P. Rwei, J. Yu, K.-Y. Lin and A. Shaju, *Process Saf. Environ. Prot.*, 2023, **172**, 986–997.
131 M. Ankitha, N. Shabana, P. V. Vaishag and P. A. Rasheed, *J. Electroanal. Chem.*, 2023, **928**, 117088.
132 C. Yuan, Z. He, Q. Chen, X. Wang, C. Zhai and M. Zhu, *Appl. Surf. Sci.*, 2021, **539**, 148241.
133 F. Shahidi and P. Ambigaipalan, *J. Funct. Foods*, 2015, **18**, 820–897.
134 J. A. Buledi, H. Shaikh, A. R. Solangi, A. Mallah, Z.-u.-H. Shah, M. M. Khan, A. L. Sanati, H. Karimi-Maleh, C. Karaman and M. B. Camarada, *Ind. Eng. Chem. Res.*, 2023, **62**, 4754–4764.
135 A. D. Chandio, A. H. Pato, I. A. Channa, S. J. Gilani, A. A. Shah, J. Ashfaq, J. A. Buledi, I. A. Chandio and M. N. B. Jumah, *Sustainability*, 2022, **14**, 14562.
136 A. F. Memon, S. Ameen, N. H. Khand, N. Qambrani, J. A. Buledi, B. Junejo, A. R. Solangi, S. I. H. Taqvi, E.-N. Dragoi and N. Zare, *Chemosphere*, 2022, **303**, 135170.
137 R. Huang, D. Liao, Z. Liu, J. Yu and X. Jiang, *Sens. Actuators, B*, 2021, **338**, 129828.
138 P. A. Rasheed, R. P. Pandey, K. A. Jabbar and K. A. Mahmoud, *J. Electroanal. Chem.*, 2021, **880**, 114934.
139 X. Wang, M. Li, S. Yang, X. Bai and J. Shan, *Microchem. J.*, 2022, **179**, 107473.
140 D. Liao, Z. Liu, R. Huang, J. Yu and X. Jiang, *Microchem. J.*, 2022, **175**, 107067.
141 V. Sanko, A. Şenocak, S. O. Tümay, Y. Orooji, E. Demirbas and A. Khataee, *Environ. Res.*, 2022, **212**, 113071.
142 J. Rajendran, T. S. Kannan, L. S. Dhanasekaran, P. Murugan, R. Atchudan, Z. A. ALOthman, M. Ouladsmane and A. K. Sundramoorthy, *Chemosphere*, 2022, **287**, 132106.
143 M. Chandran, E. Aswathy, I. Shamna, M. Vinoba, R. Kottappara and M. Bhagiyalakshmi, *Mater. Today: Proc.*, 2021, **46**, 3136–3143.
144 R. Huang, D. Liao, S. Chen, J. Yu and X. Jiang, *Sens. Actuators, B*, 2020, **320**, 128386.
145 K. S. Ranjith, A. E. Vilian, S. M. Ghoreishian, R. Umapathi, S.-K. Hwang, C. W. Oh, Y. S. Huh and Y.-K. Han, *J. Hazard. Mater.*, 2022, **421**, 126775.
146 T. Yu, S. Li, L. Zhang, F. Li, J. Wang, H. Pan and D. Zhang, *J. Colloid Interface Sci.*, 2023, **629**, 546–558.